FD5180, a novel protein kinase affinity probe and the effect of bead loading on protein kinases identification

Fiona M. Deane,[a†] Andrew J. S. Lin,[a†] Peter G Hains,[b†] Sarah L. Pilgrim,[a] Phillip J Robinson[b] and Adam McCluskey[a*]

[a] Chemistry, Centre for Chemical Biology, The University of Newcastle, University Drive, Callaghan NSW 2308 Australia. Phone: +61 249 216486; Fax: +61 249 215472; Email: Adam.McCluskey@newcastle.edu.au

[b] Cell Signalling Unit, Children's Medical Research Institute, The University of Sydney, Sydney, NSW 2145, Australia.

[†]Contributed equally to this project.

Table of Contents

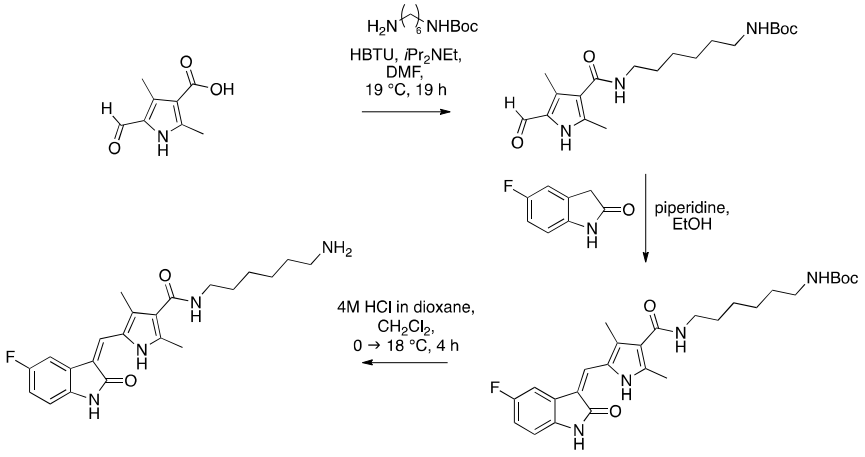

Scheme S1: Synthetic Sequence of Modified Sunitnib

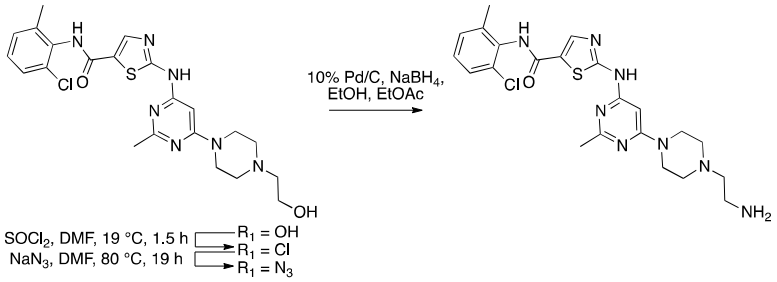

Scheme S2: Synthetic Sequence of Modified Dasatanib

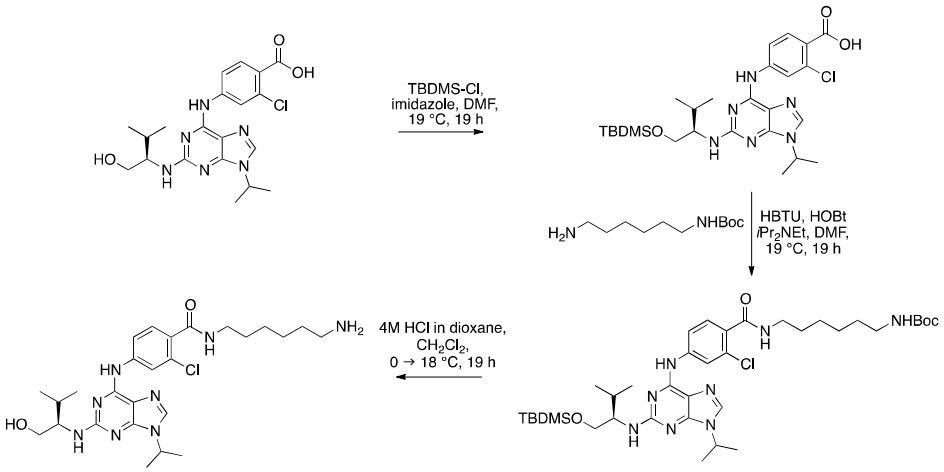

Scheme S3: Synthetic Sequence of Modified Purvalanol B

Table S1. Background protein numbers determined after bead exposure to HeLa cell lysate.

Loading (%)	BIMX (S1) No. proteins	CZC8004 (S2) No. proteins
0.1	915	1657
0.5	832	755
1	895	902
2	949	726
5	1214	1083
10	1176	961
25	1221	1235
50	1415	1374
Proteins common to all loadings	369	322
Proteins common to all S1 and S2 loadings	273	
Proteins common to S1, S2 and blank	271	

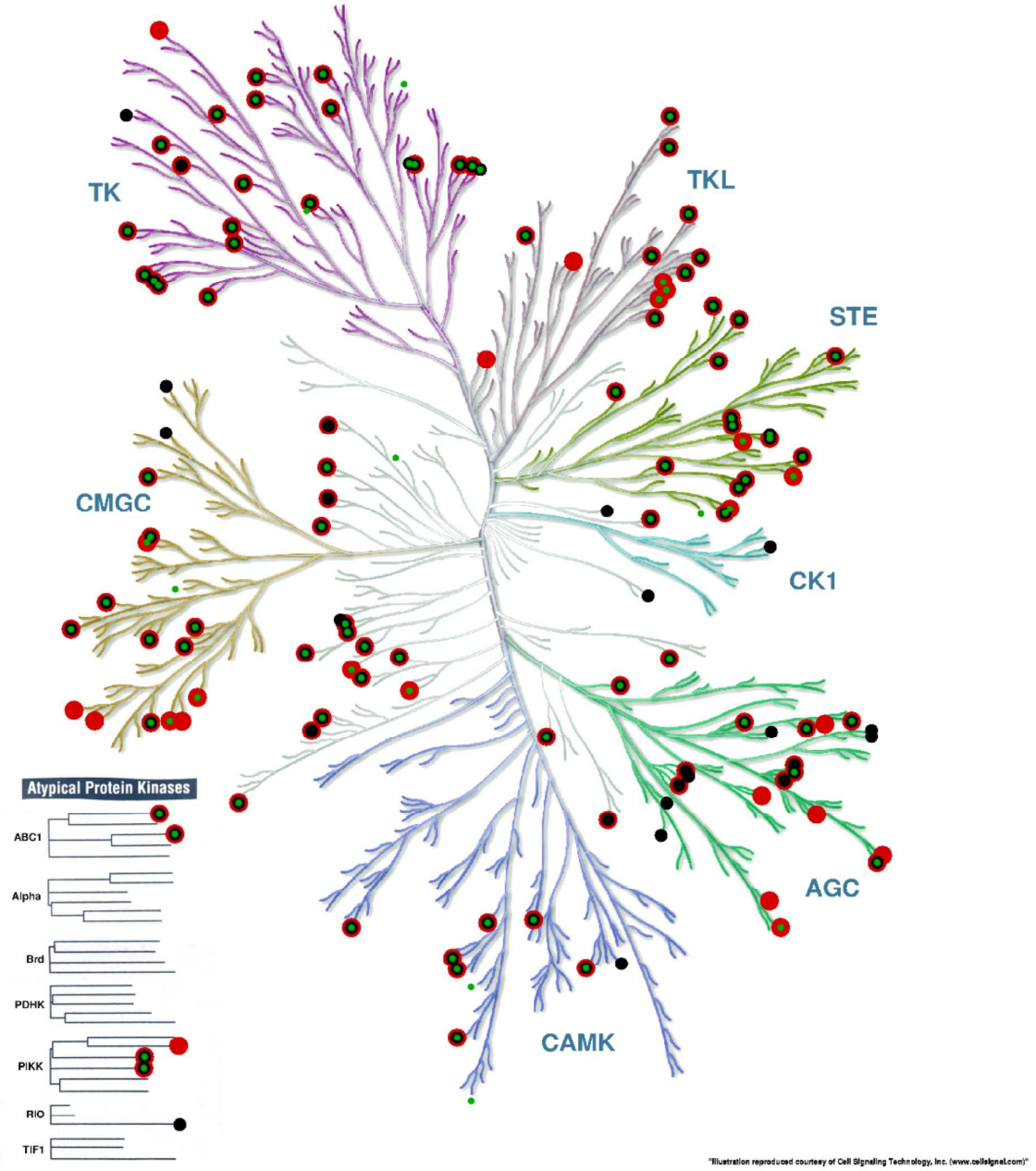

Figure S1: Comparison of protein kinases pulled down using the CTX-0294885 (**S9**, black), KC19 (**S10**, green) and hybrid (**S15**, red) kinase affinity beads. Illustration reproduced courtesy of Cell Signalling Technology, Inc. www.cellsignal.com).

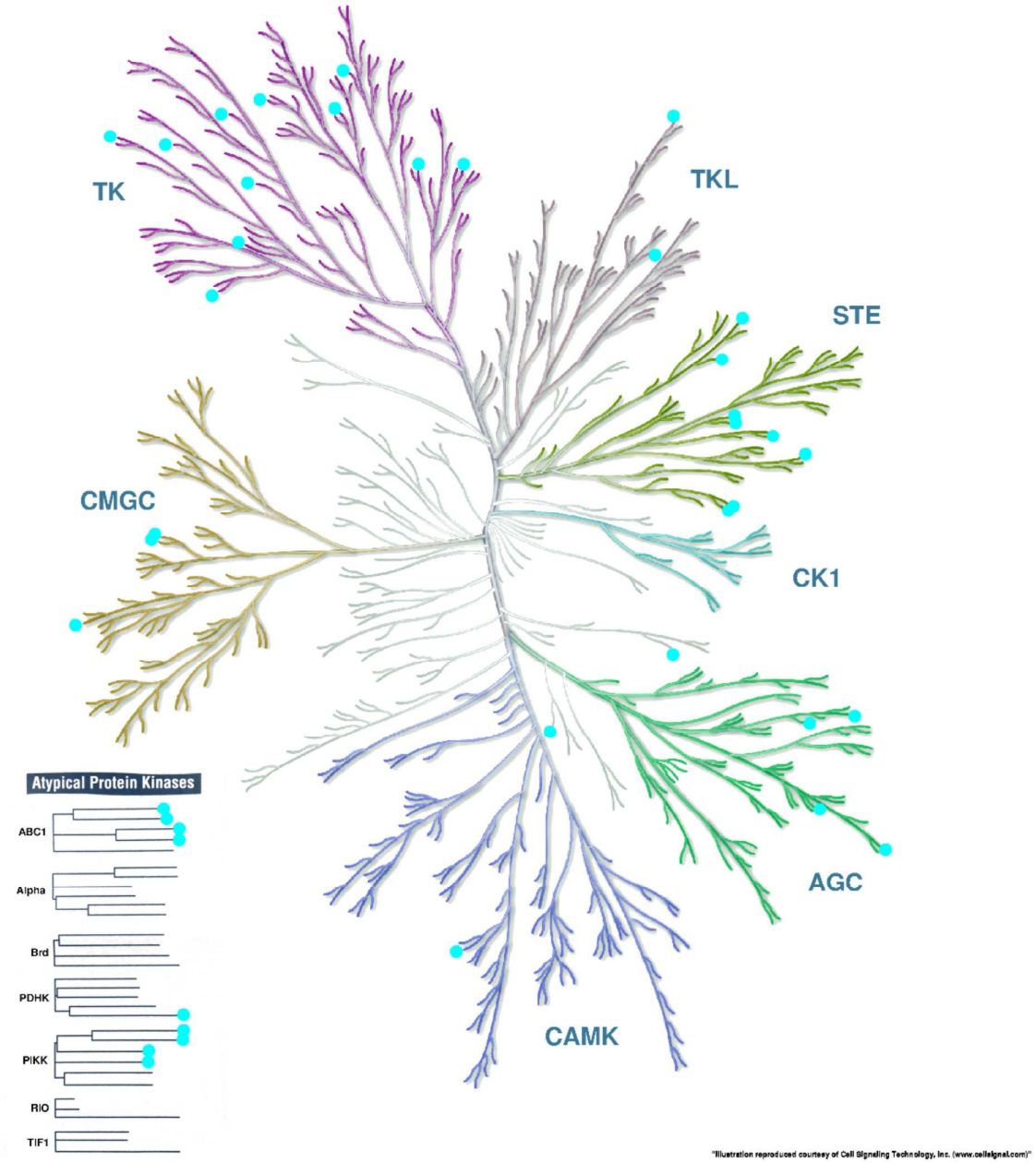

Figure S2: Comparison of protein kinases pulled down using BIMX (**S1**) kinase affinity beads. Illustration reproduced courtesy of Cell Signalling Technology, Inc. www.cellsignal.com).

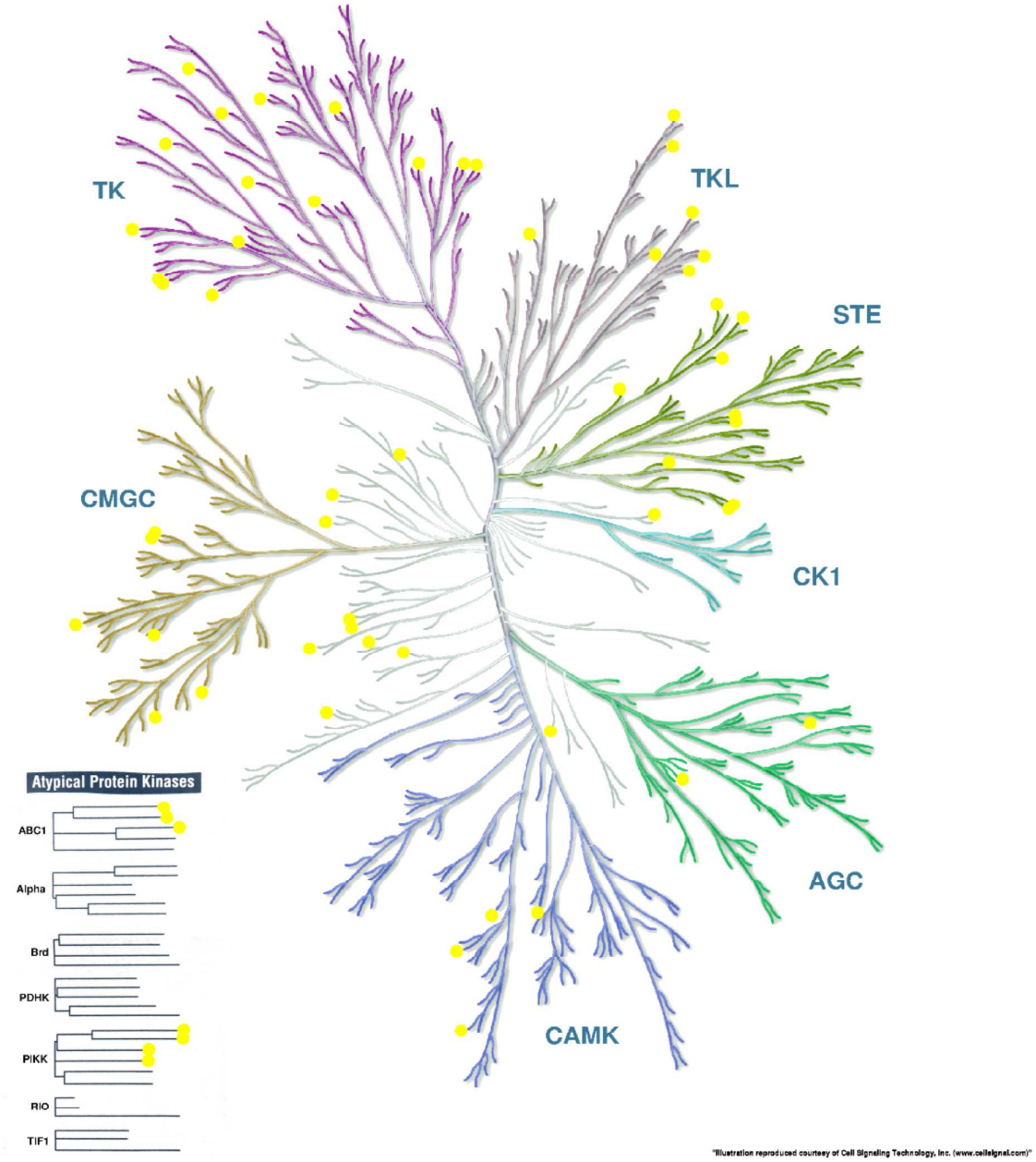

Figure S3: Comparison of protein kinases pulled down using CZC8004 (**S2**) kinase affinity beads. Illustration reproduced courtesy of Cell Signalling Technology, Inc. www.cellsignal.com).

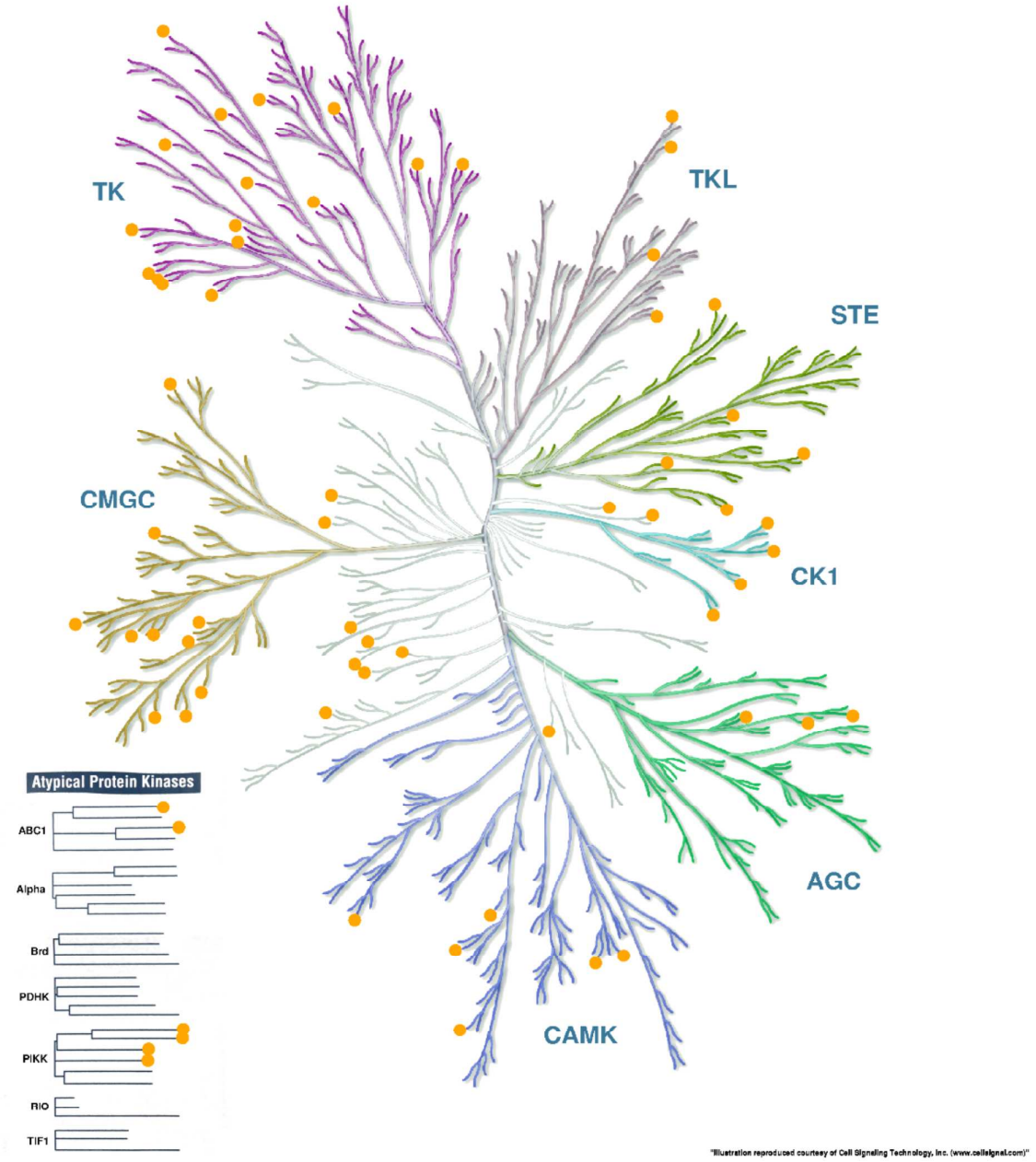

Figure S4: Comparison of protein kinases pulled down using Purvalanol B (**S6**) kinase affinity beads. Illustration reproduced courtesy of Cell Signalling Technology, Inc. www.cellsignal.com).

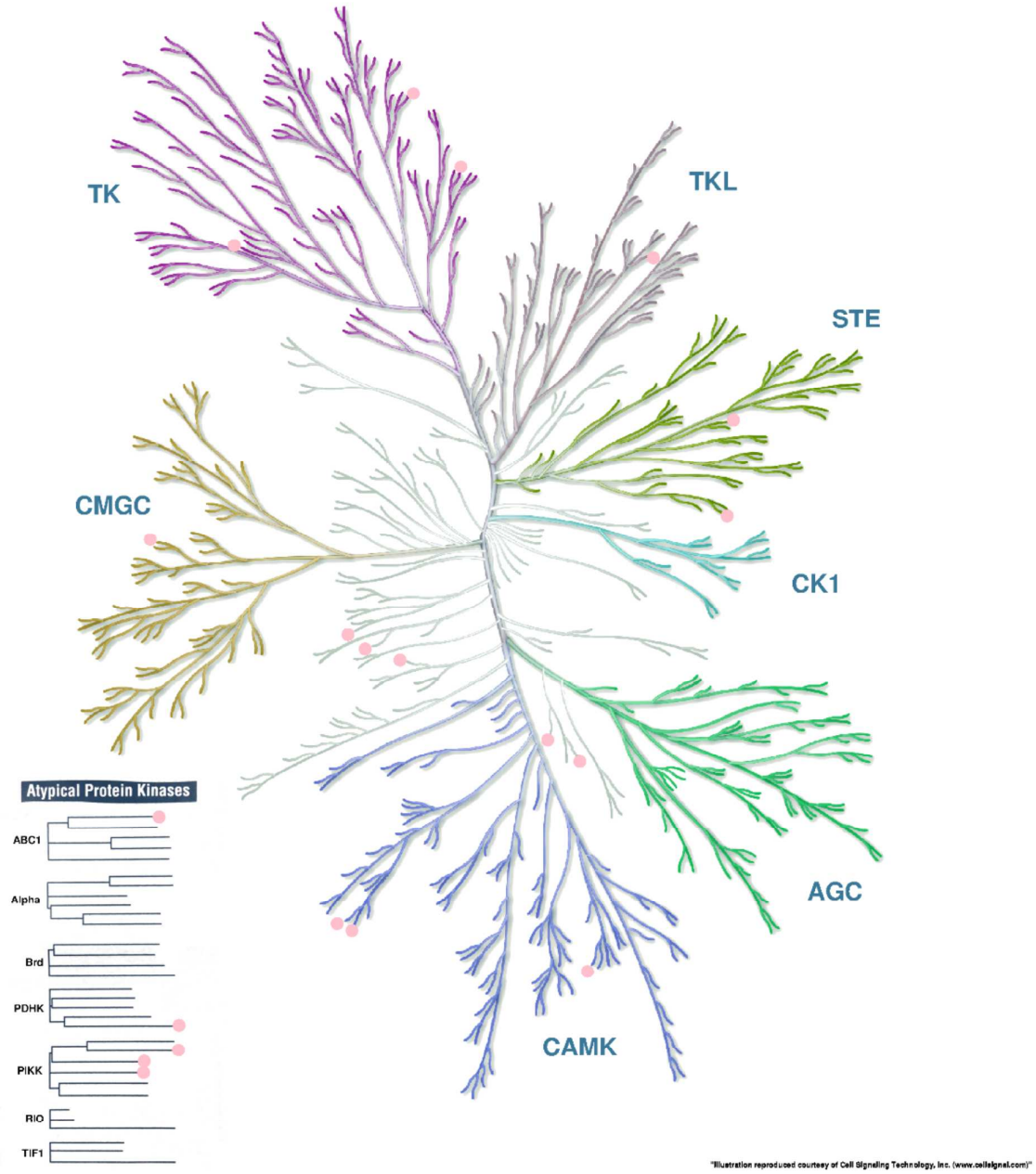

Figure S5: Comparison of protein kinases pulled down using Sunitinib (**S7**) kinase affinity beads. Illustration reproduced courtesy of Cell Signalling Technology, Inc. www.cellsignal.com).

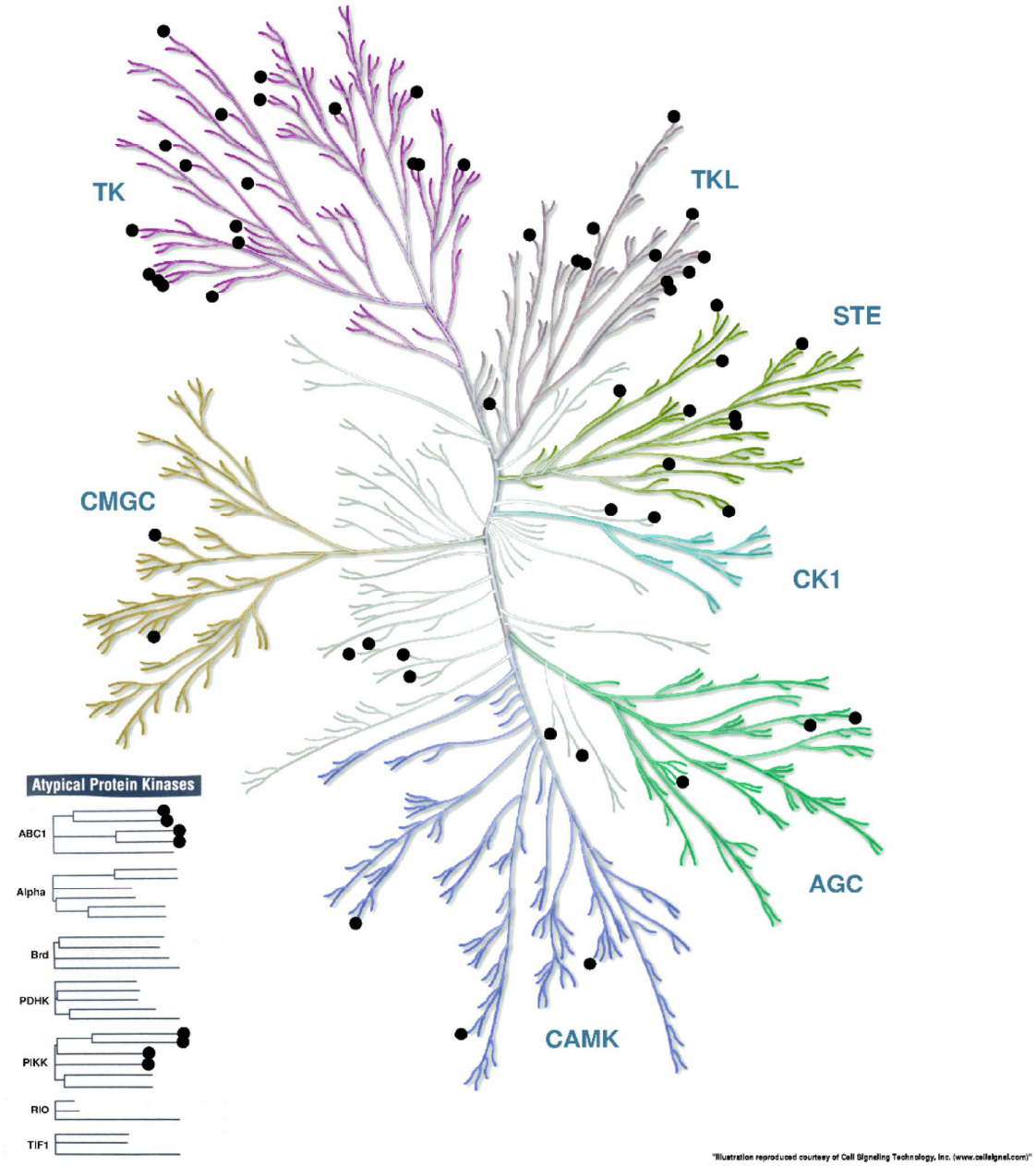

Figure S6: Comparison of protein kinases pulled down using Dasitinib (**S8**) kinase affinity beads. Illustration reproduced courtesy of Cell Signalling Technology, Inc. www.cellsignal.com).

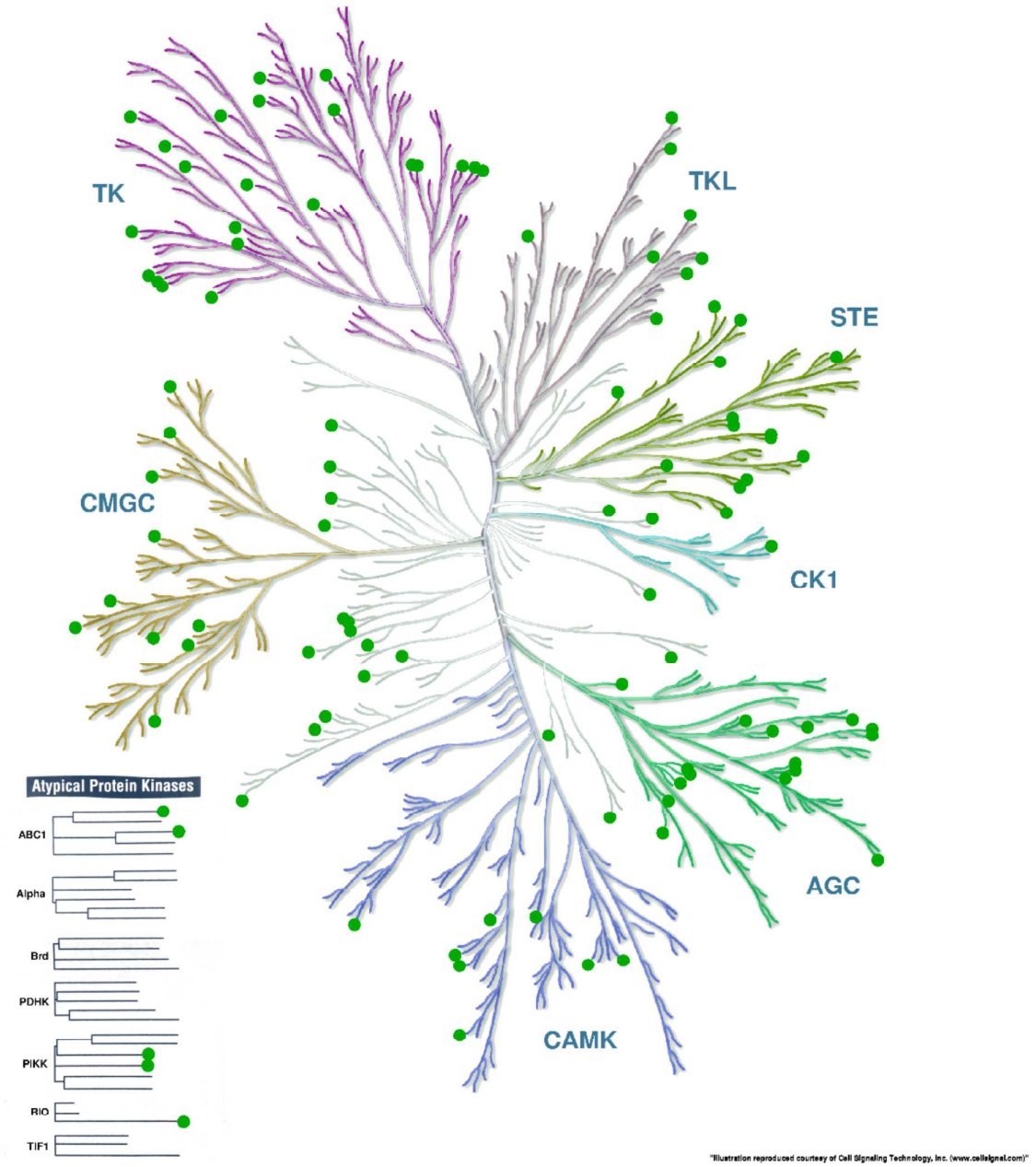

Figure S7: Comparison of protein kinases pulled down using CTx-0294885 (**S9**) kinase affinity beads. Illustration reproduced courtesy of Cell Signalling Technology, Inc. www.cellsignal.com).

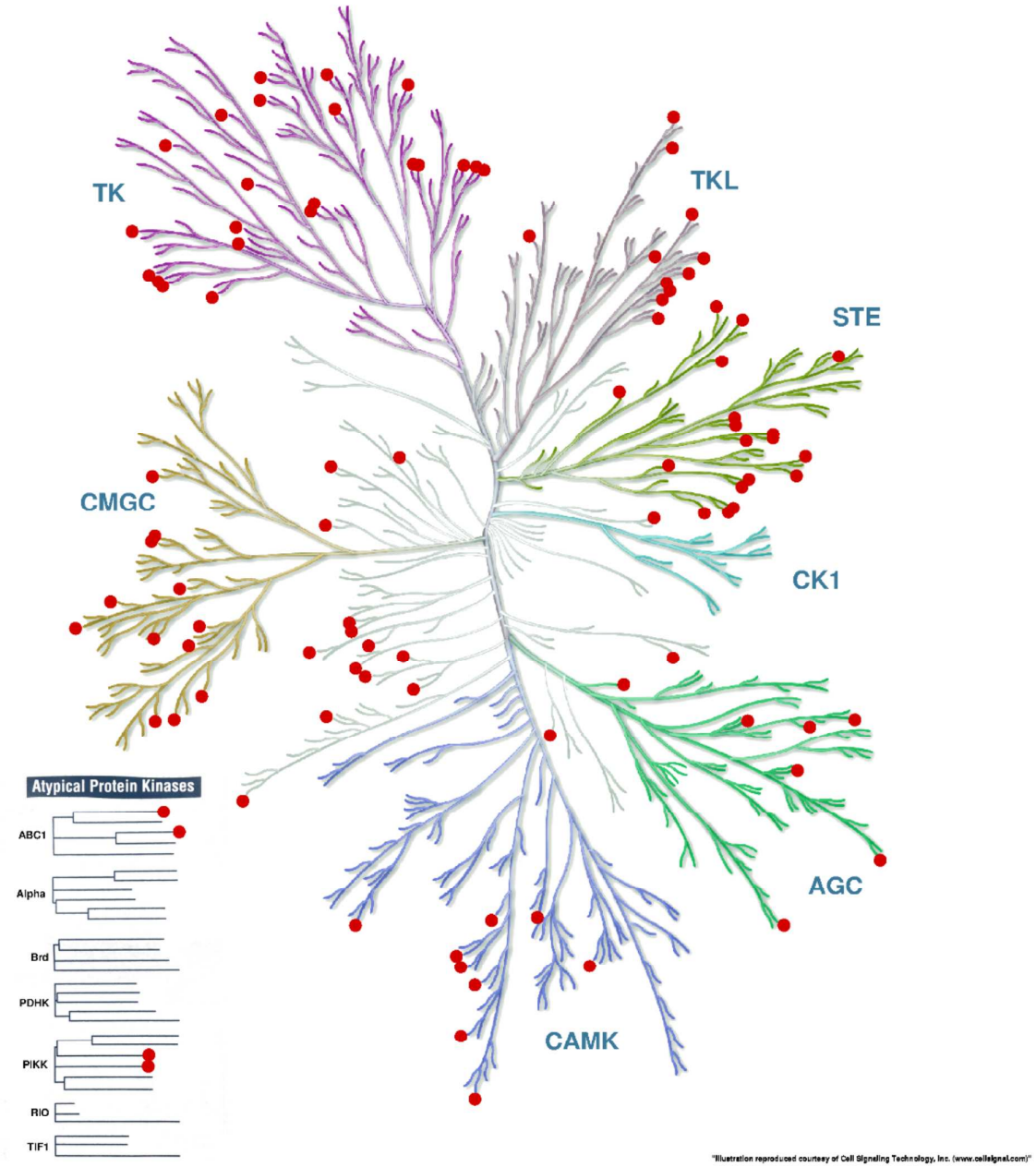

Figure S8: Comparison of protein kinases pulled down using Kuster Compound 19 (**S10**) kinase affinity beads. Illustration reproduced courtesy of Cell Signalling Technology, Inc. www.cellsignal.com).

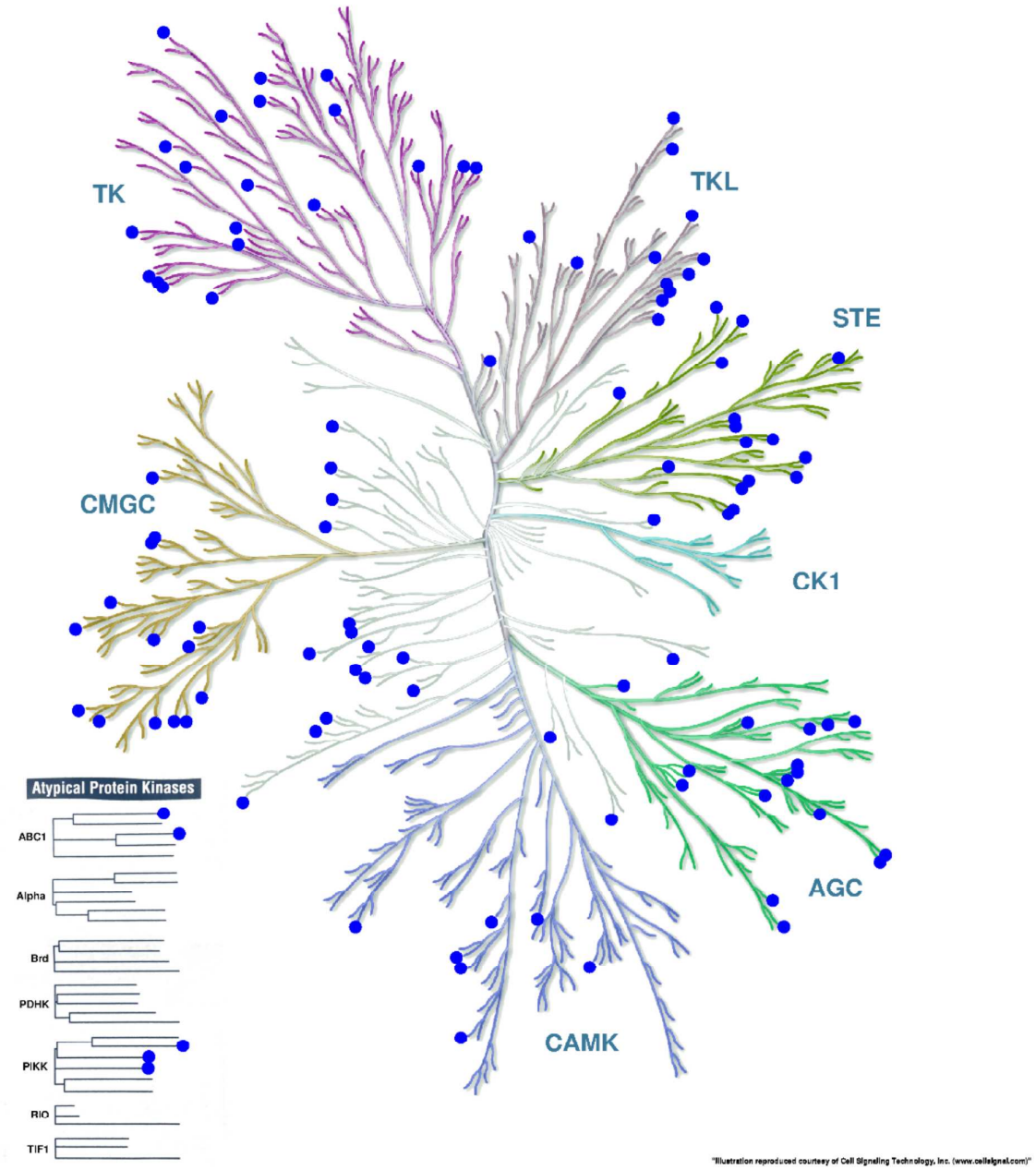

Figure S9: Comparison of protein kinases pulled down using FD5180 (**S15**) kinase affinity beads. Illustration reproduced courtesy of Cell Signalling Technology, Inc. www.cellsignal.com).

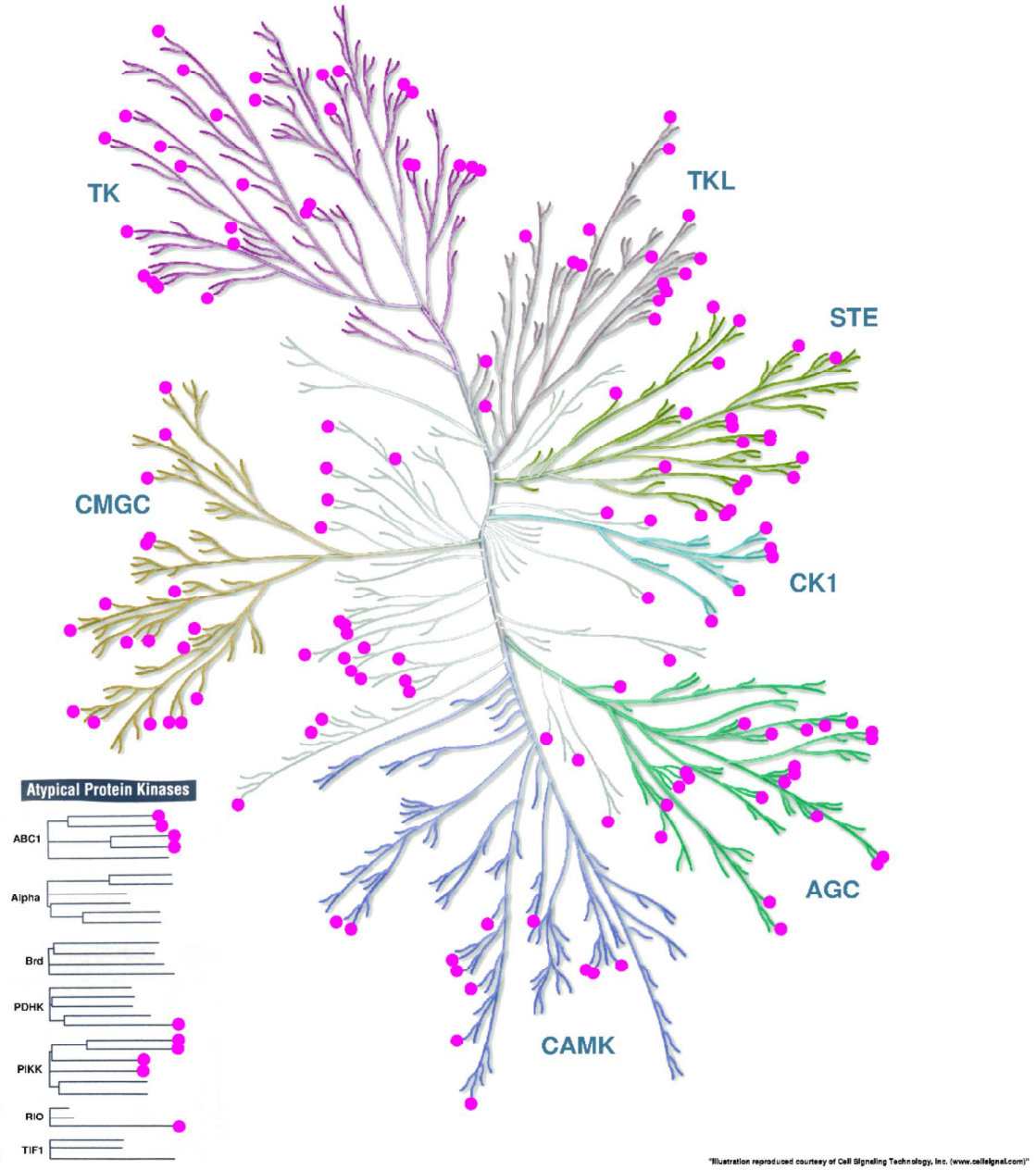

Figure S10: Comparison of protein kinases pulled down using all kinase affinity beads from SF1-SF9. Illustration reproduced courtesy of Cell Signalling Technology, Inc. www.cellsignal.com).

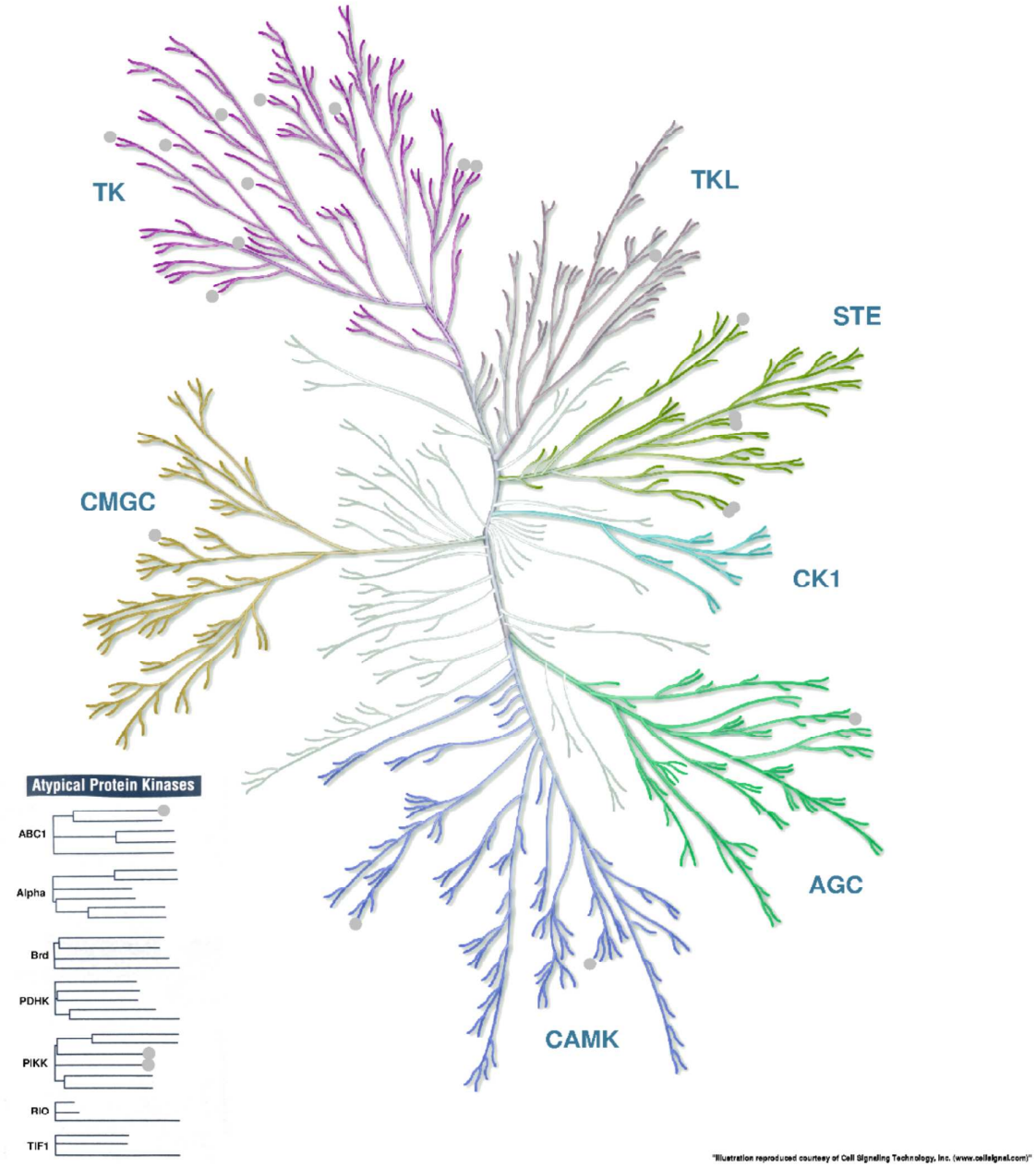

Figure S11: Comparison of protein kinases pulled down using blank (control) kinase affinity beads. Illustration reproduced courtesy of Cell Signalling Technology, Inc. www.cellsignal.com).

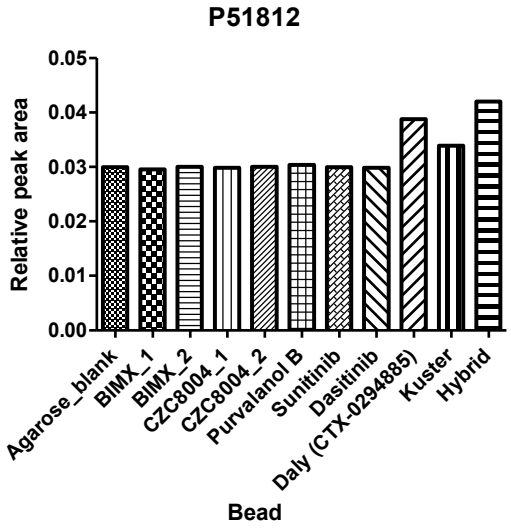

Figure S12: Bead binding profile for protein P51812. The relative amount of P51812 (Ribosomal protein S6 kinase alpha-3) bound to each bead tested in the study.

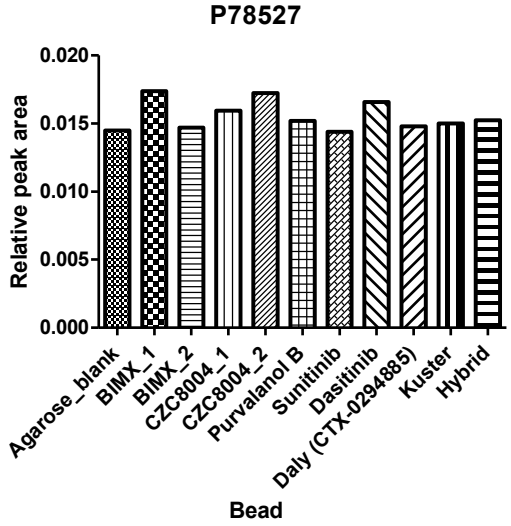

Figure S13: Bead binding profile for protein P78527. The relative amount of P78527 (DNA-dependent protein kinase catalytic subunit) bound to each bead tested in the study.

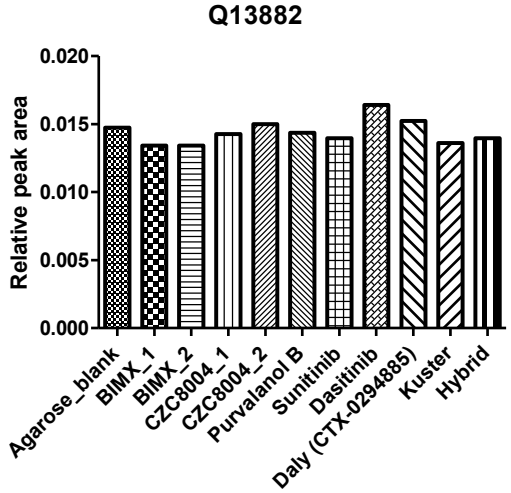

Figure S14: Bead binding profile for protein Q13882. The relative amount of Q13882 (Protein-tyrosine kinase 6) bound to each bead tested in the study.

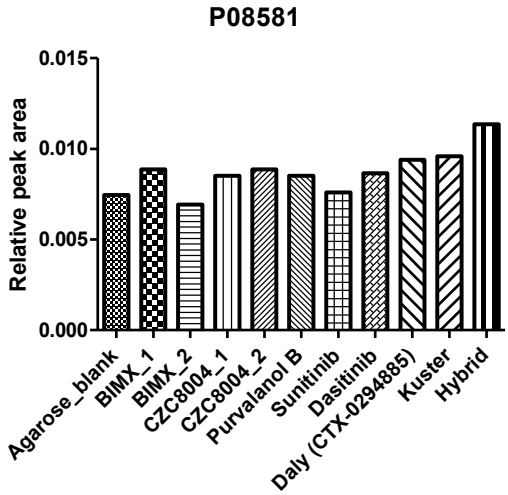

Figure S15: Bead binding profile for protein P08581. The relative amount of P08581 (Hepatocyte growth factor receptor) bound to each bead tested in the study.

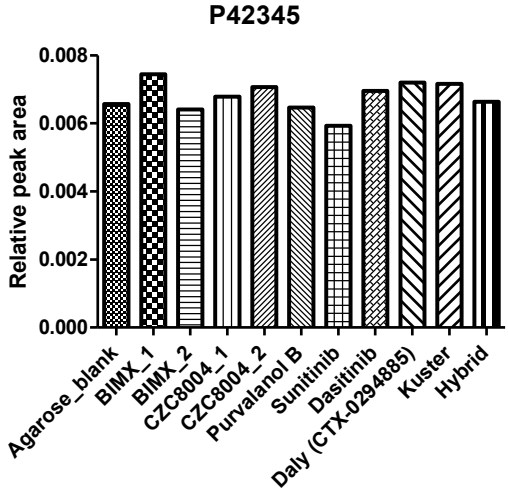

Figure S16: Bead binding profile for protein P42345. The relative amount of P42345 (Serine/threonine-protein kinase mTOR) bound to each bead tested in the study.

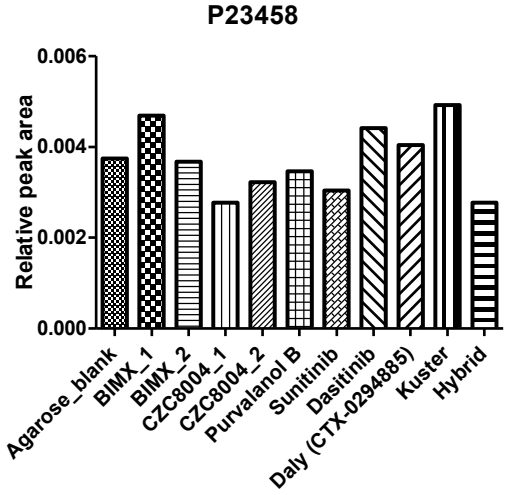

Figure S17: Bead binding profile for protein P23458. The relative amount of P23458 (Tyrosine-protein kinase JAK1) bound to each bead tested in the study.

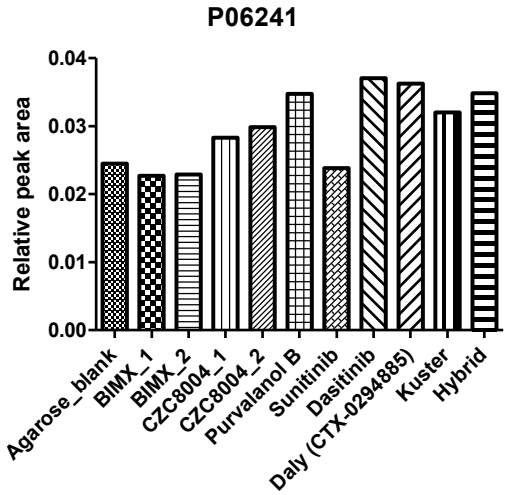

Figure S18: Bead binding profile for protein P06241. The relative amount of P06241 (Tyrosine-protein kinase Fyn) bound to each bead tested in the study.

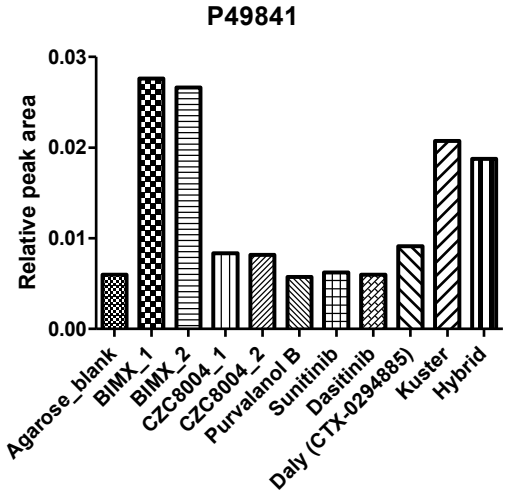

Figure S19: Bead binding profile for protein P49841. The relative amount of P49841 (Glycogen synthase kinase-3 beta) bound to each bead tested in the study.

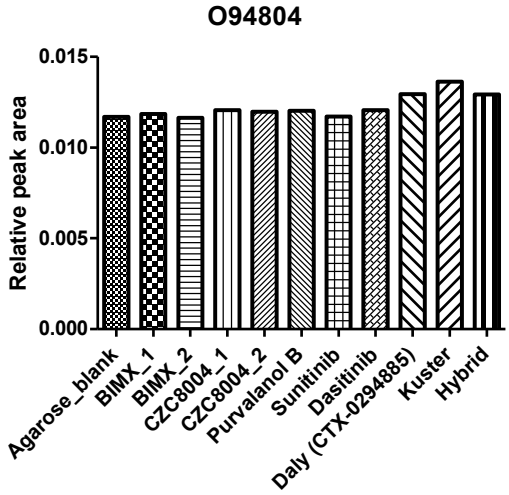

Figure S20: Bead binding profile for protein O94804. The relative amount of O94804 (Serine/threonine-protein kinase 10) bound to each bead tested in the study.

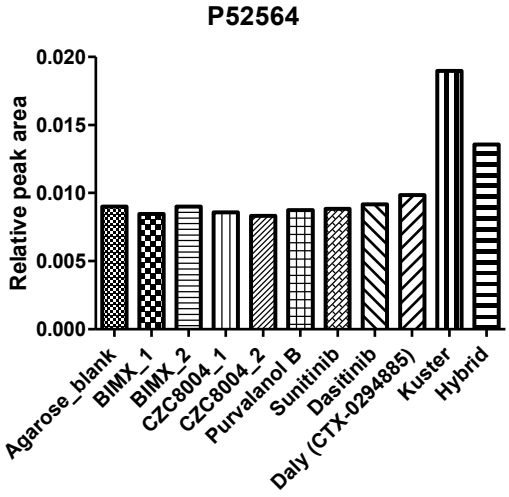

Figure S21: Bead binding profile for protein P52564. The relative amount of P52564 (Dual specificity mitogen-activated protein kinase 6) bound to each bead tested in the study.

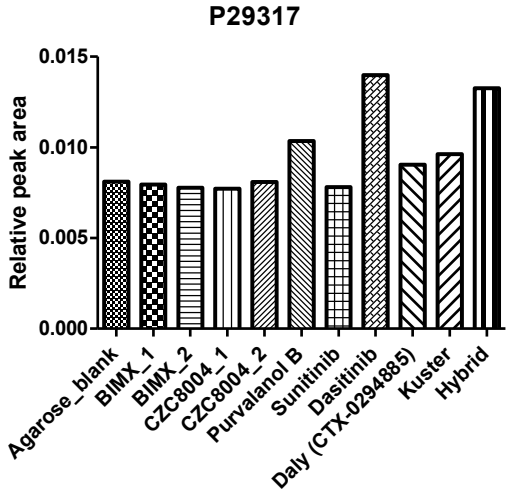

Figure S22: Bead binding profile for protein P29317. The relative amount of P29317 (Ephrin type-A receptor 2) bound to each bead tested in the study.

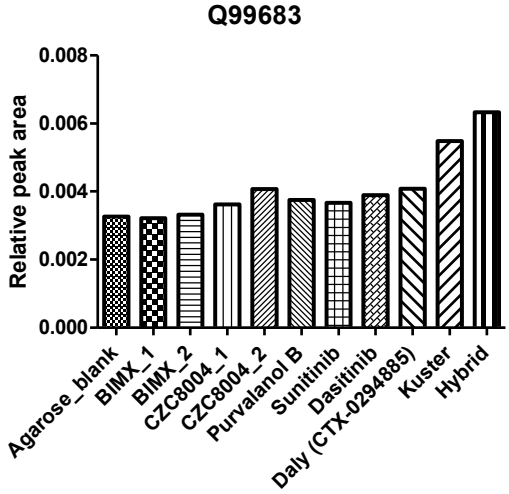

Figure S23: Bead binding profile for protein Q99683. The relative amount of Q99683 (Mitogen-activated protein kinase kinase 5) bound to each bead tested in the study.

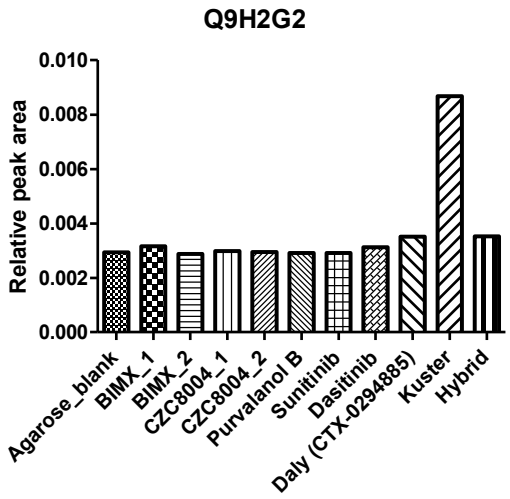

Figure S24: Bead binding profile for protein Q9H2G2. The relative amount of Q9H2G2 (STE20-like serine/threonine-protein kinase) bound to each bead tested in the study.

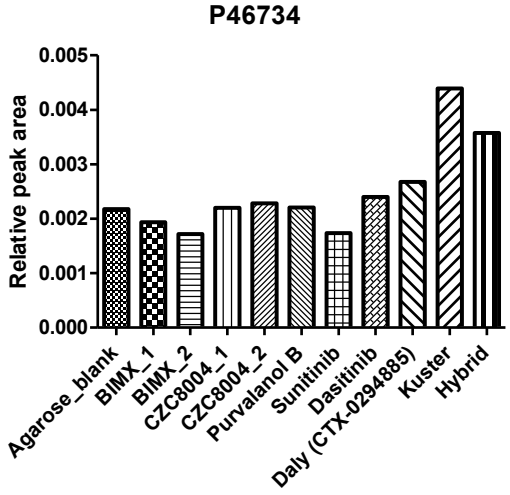

Figure S25: Bead binding profile for protein P46734. The relative amount of P46734 (Dual specificity mitogen-activated protein kinase 3) bound to each bead tested in the study.

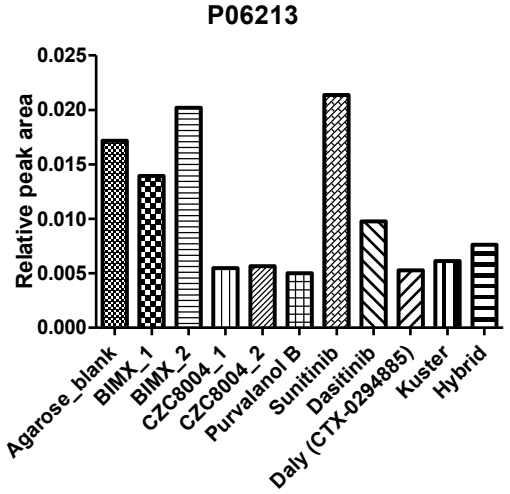

Figure S26: Bead binding profile for protein P06213. The relative amount of P06213 (Insulin receptor) bound to each bead tested in the study.

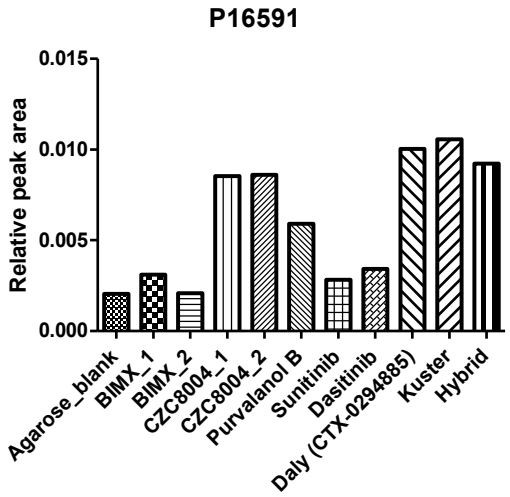

Figure S27: Bead binding profile for protein P16591. The relative amount of P16591 (Tyrosine-protein kinase Fer) bound to each bead tested in the study.

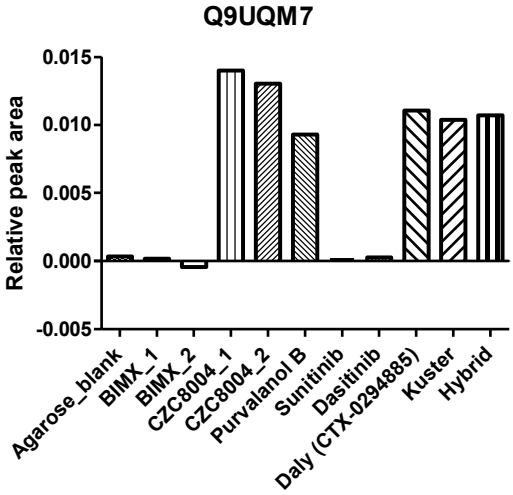

Figure S28: Bead binding profile for protein Q9UQM7. The relative amount of Q9UQM7 (Calcium/calmodulin-dependent protein kinase type II subunit alpha) bound to each bead tested in the study.

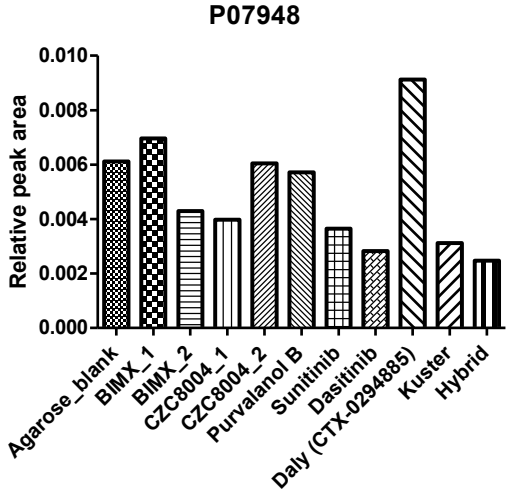

Figure S29: Bead binding profile for protein P07948. The relative amount of P07948 (Tyrosine-protein kinase Lyn) bound to each bead tested in the study.

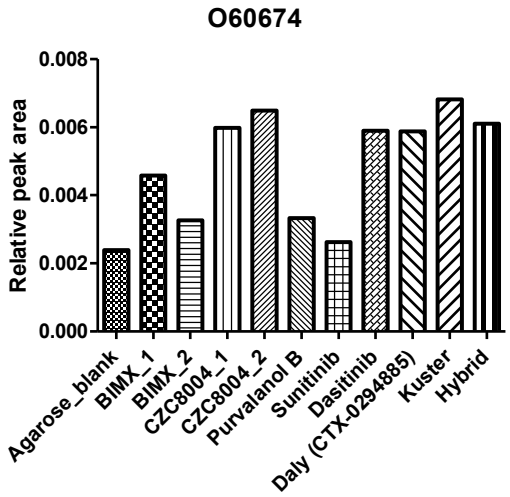

Figure S30: Bead binding profile for protein O60674. The relative amount of O60674 (Tyrosine-protein kinase JAK2) bound to each bead tested in the study.

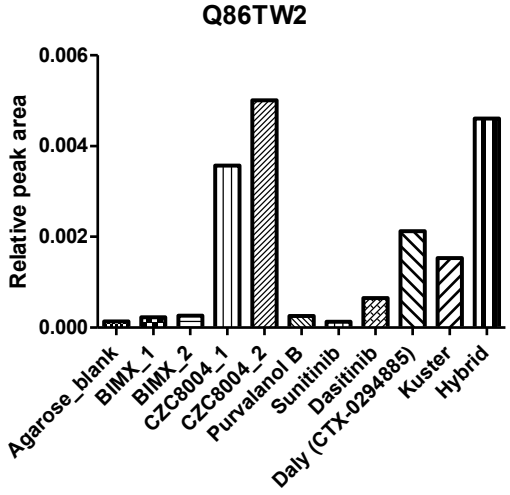

Figure S31: Bead binding profile for protein Q86TW2. The relative amount of Q86TW2 (Uncharacterised aarF domain-containing protein kinase 1) bound to each bead tested in the study.

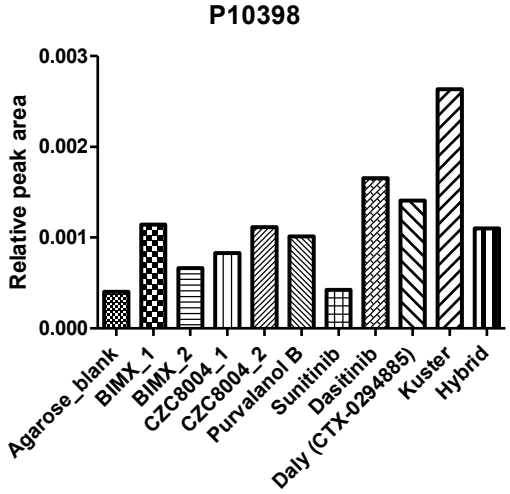

Figure S32: Bead binding profile for protein P10398. The relative amount of P10398 (Serine/threonine-protein kinase A-Raf) bound to each bead tested in the study.

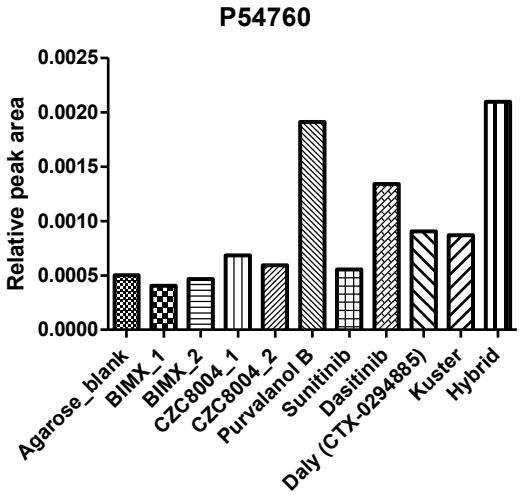

Figure S33: Bead binding profile for protein P54760. The relative amount of P54760 (Ephrin type-B receptor 4) bound to each bead tested in the study.

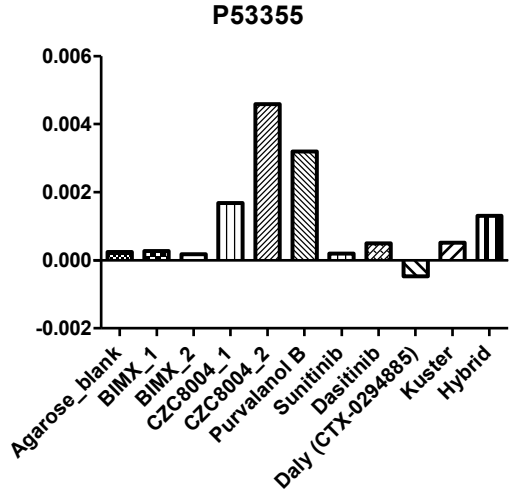

Figure S34: Bead binding profile for protein P53355. The relative amount of P53355 (Death-associated protein kinase 1) bound to each bead tested in the study.

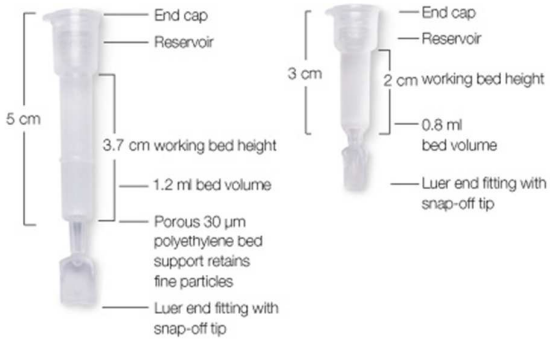

Figure S35. Mini Bio-Spin Chromatography Columns for coupling reactions

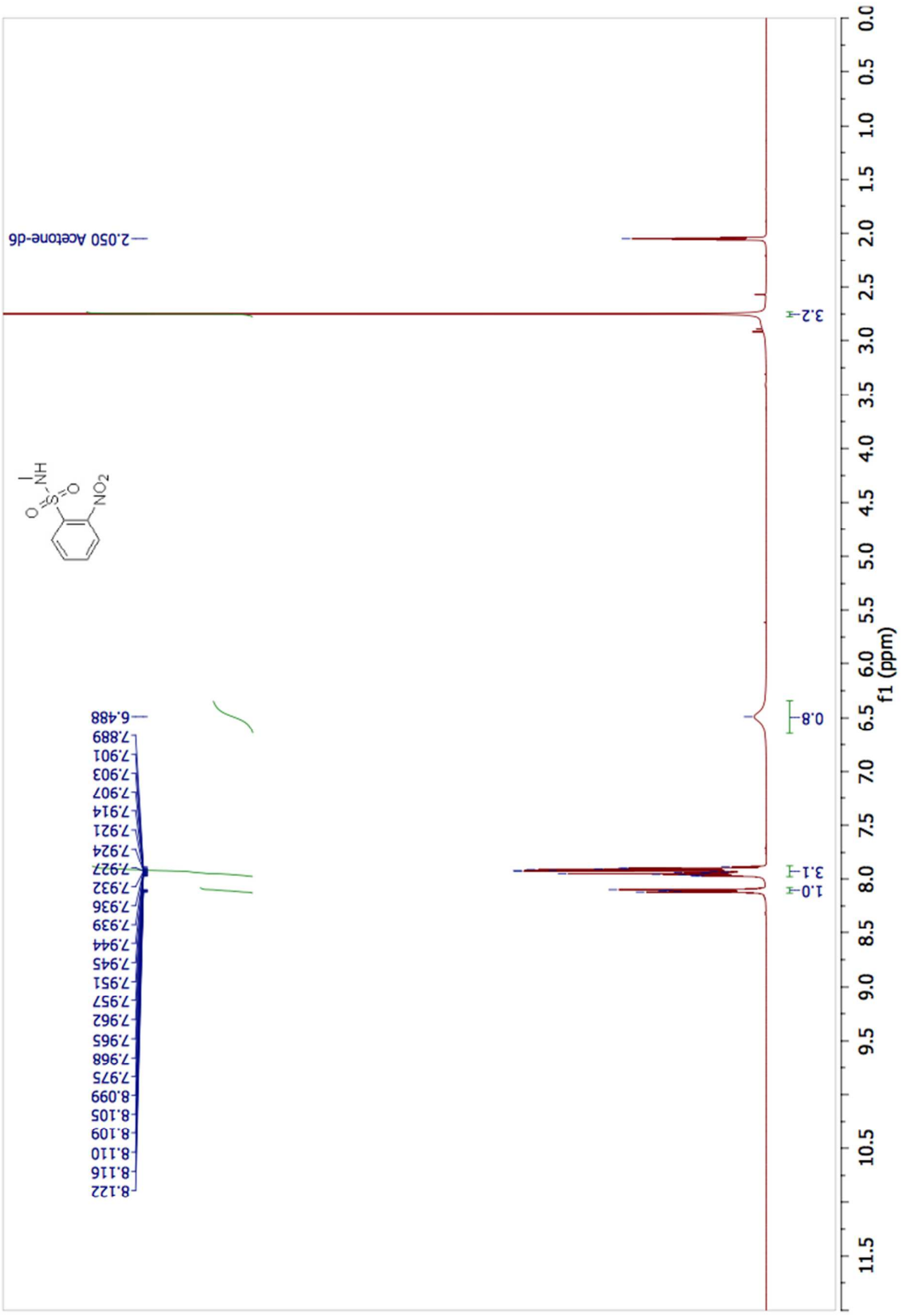

Figure S36: ^{1}H NMR spectrum of **12**.

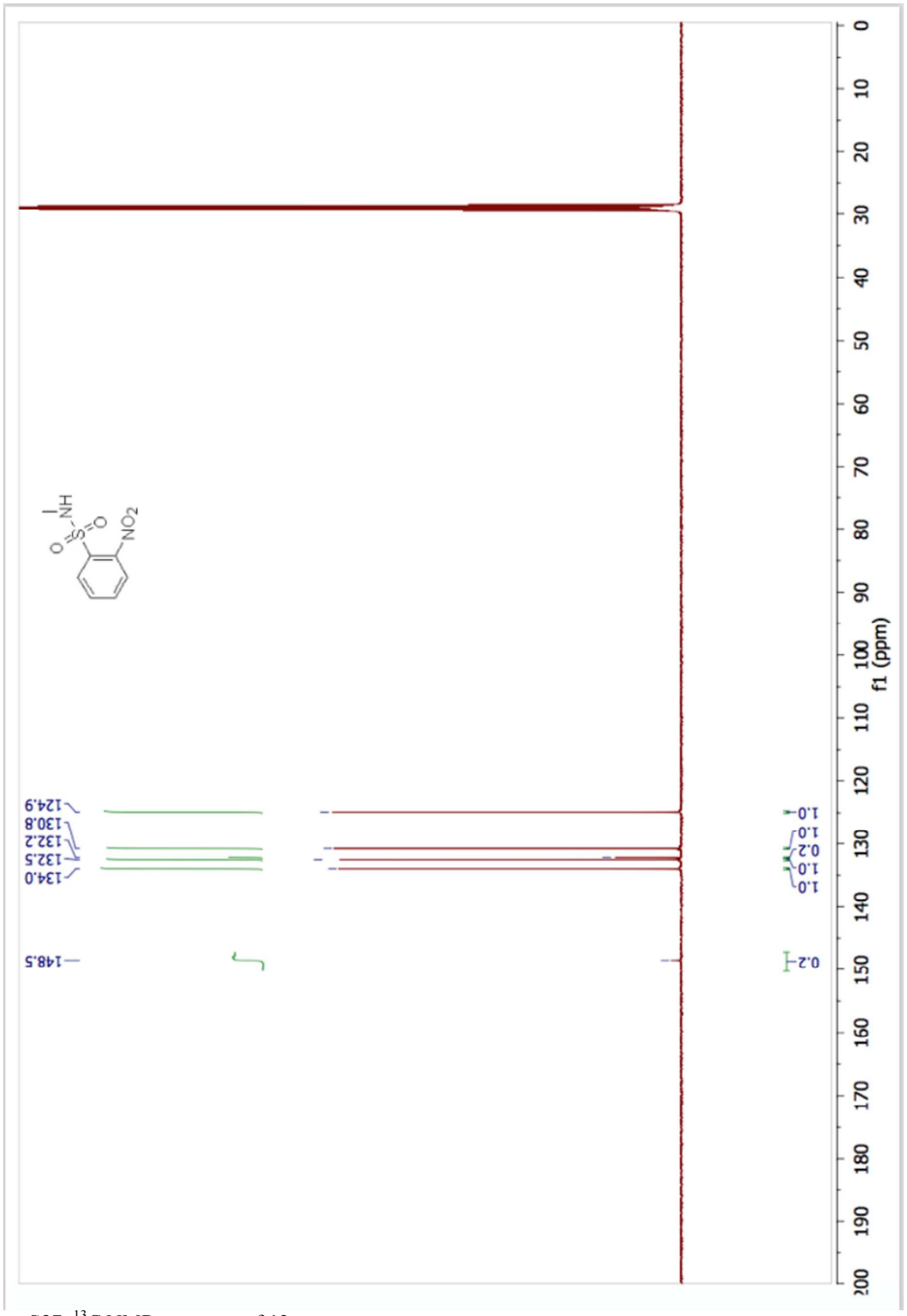

Figure S37: ^{13}C NMR spectrum of **12**.

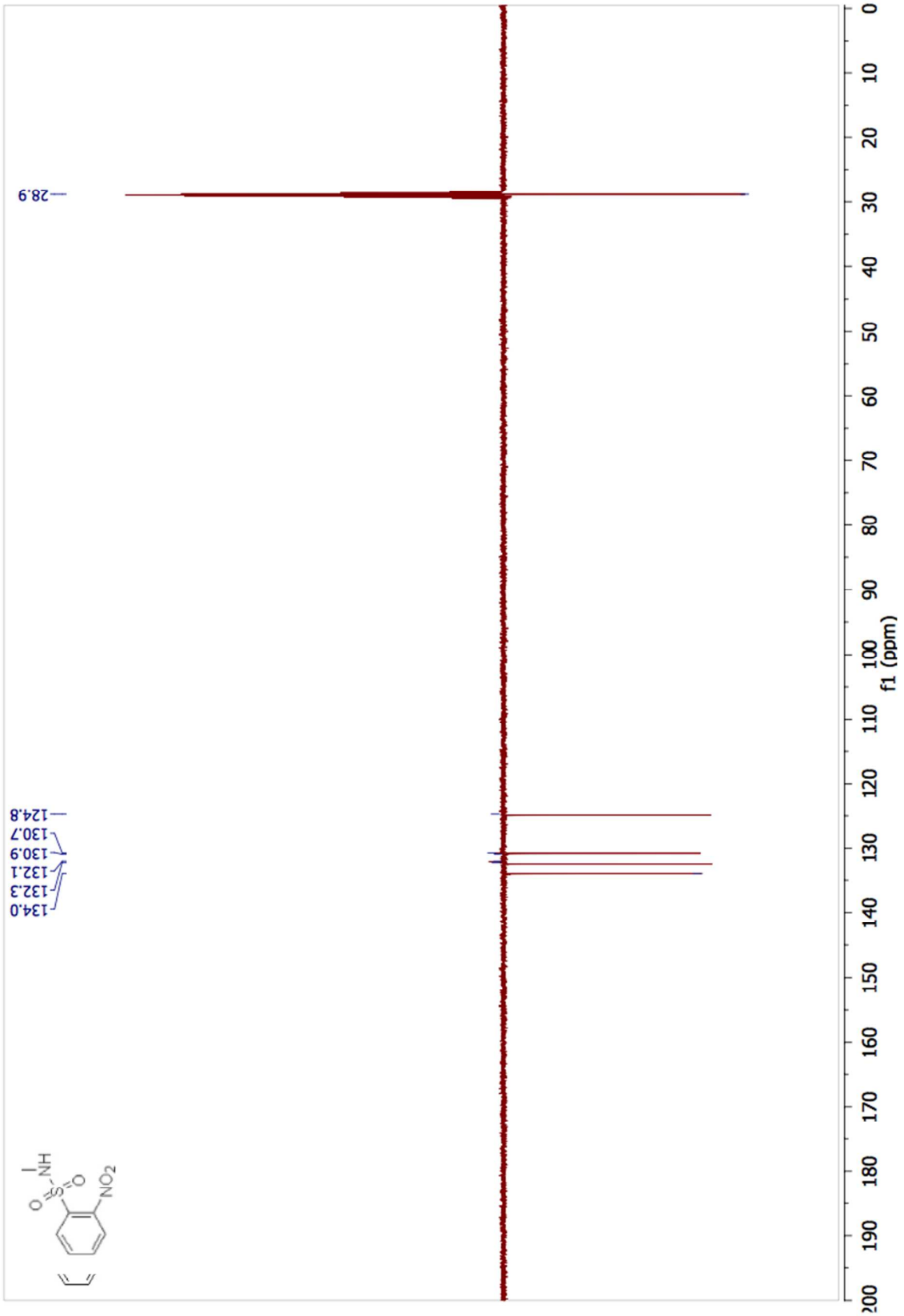

Figure S38: DEPT NMR spectrum of **12**.

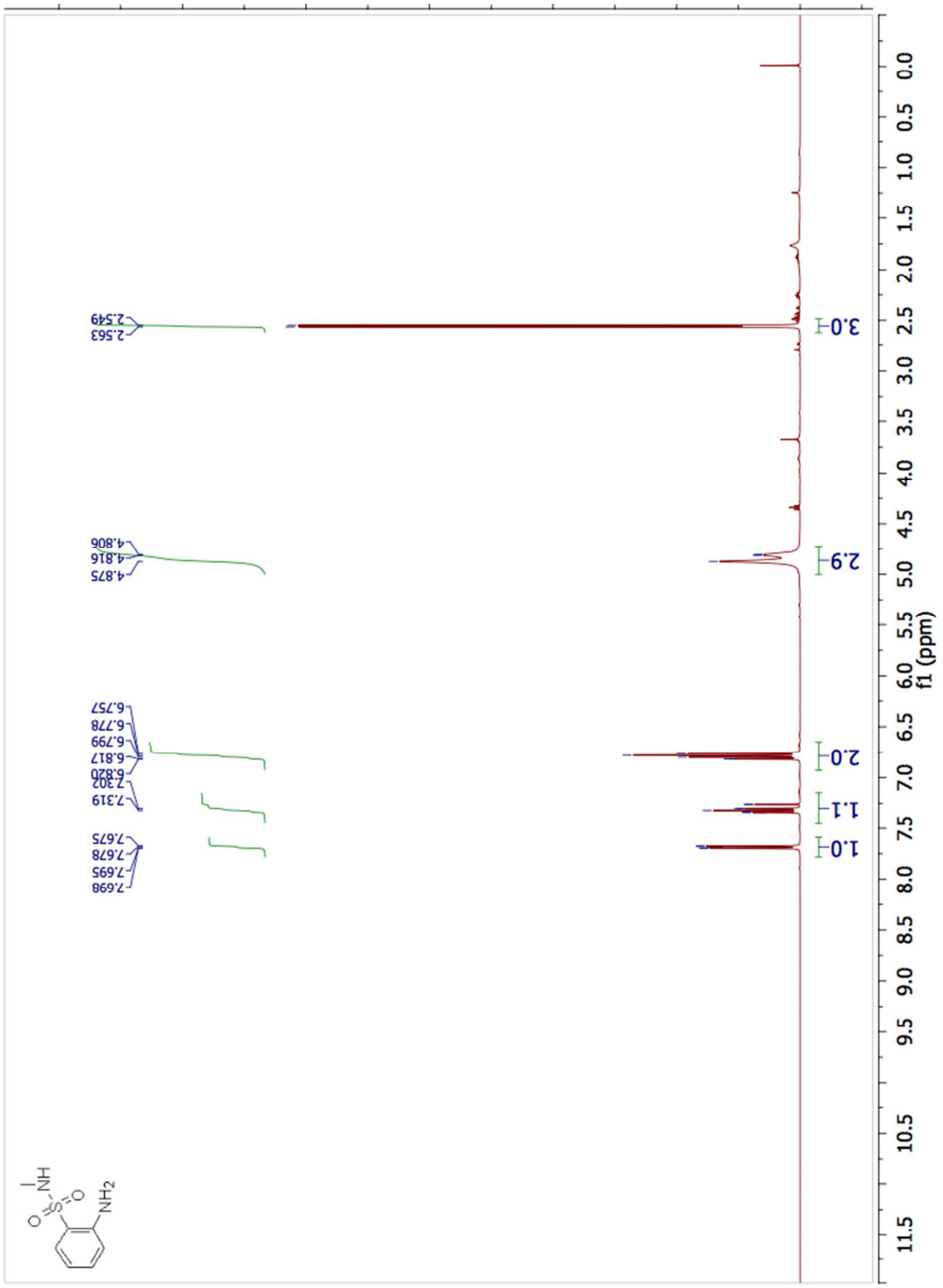

Figure S39: ^{1}H NMR spectrum of **13**.

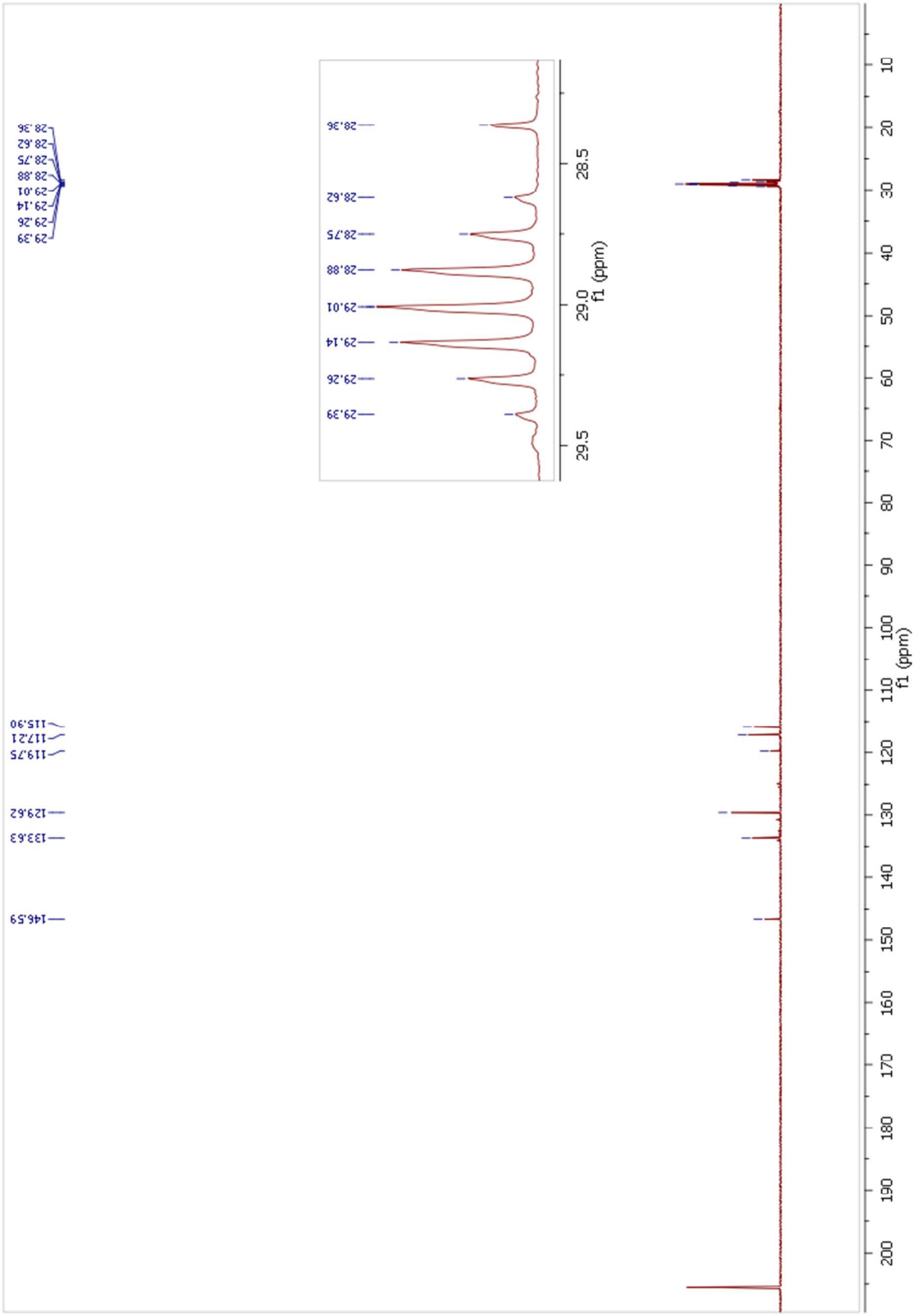

Figure S40: ^{13}C NMR spectrum of **13**.

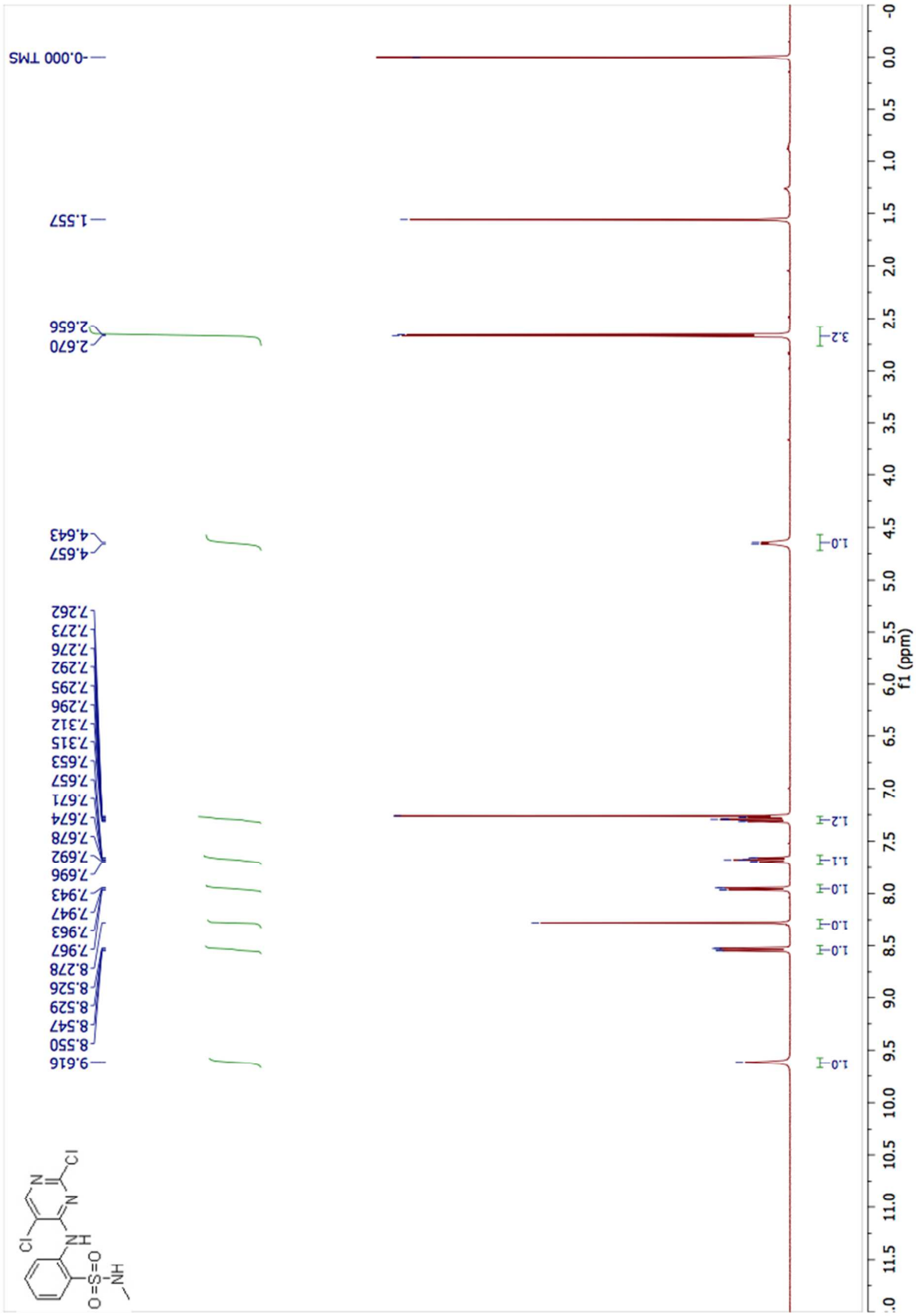

Figure S41: ^{1}H NMR spectrum of **14**.

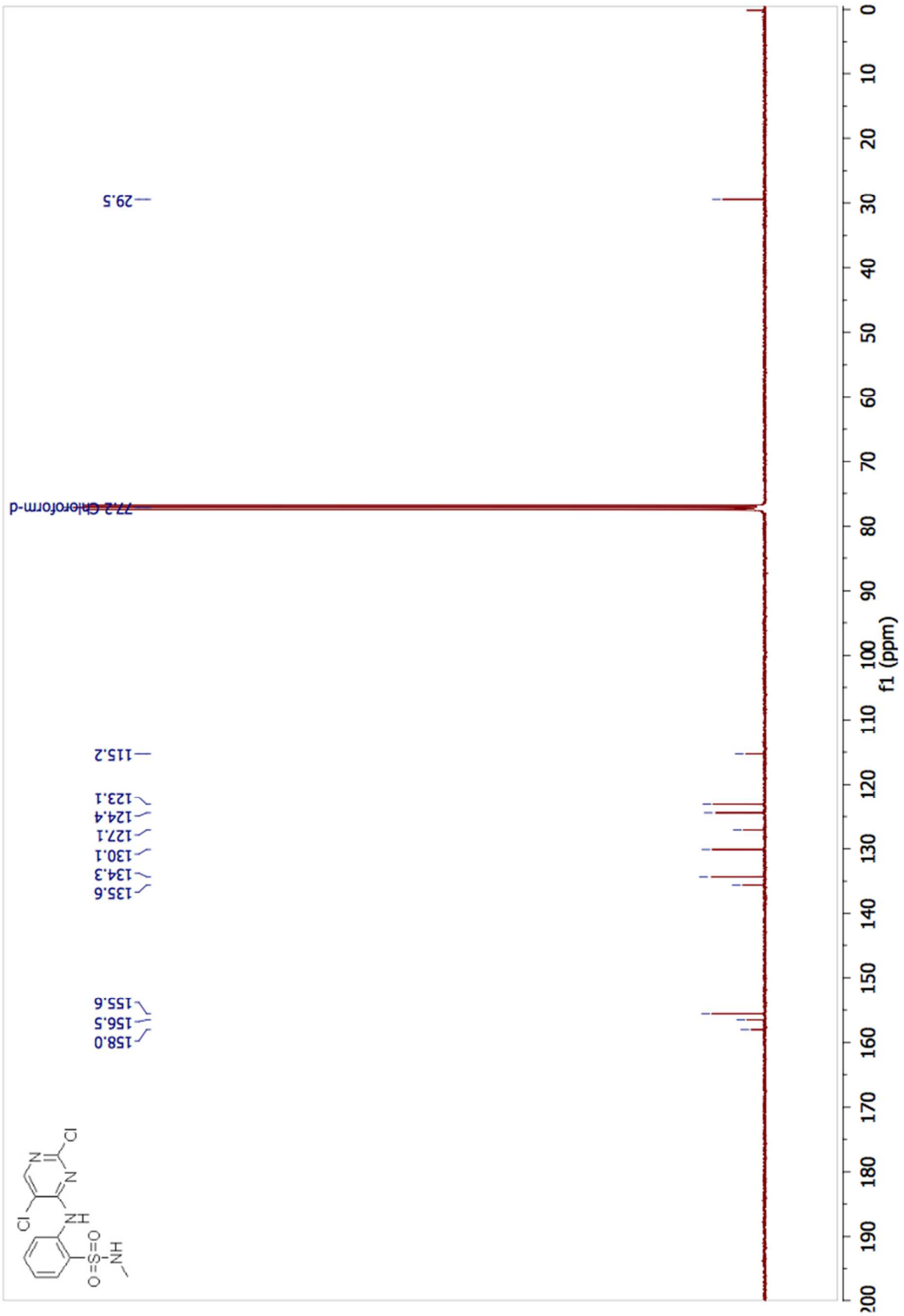

Figure S42: ^{13}C NMR spectrum of **14**.

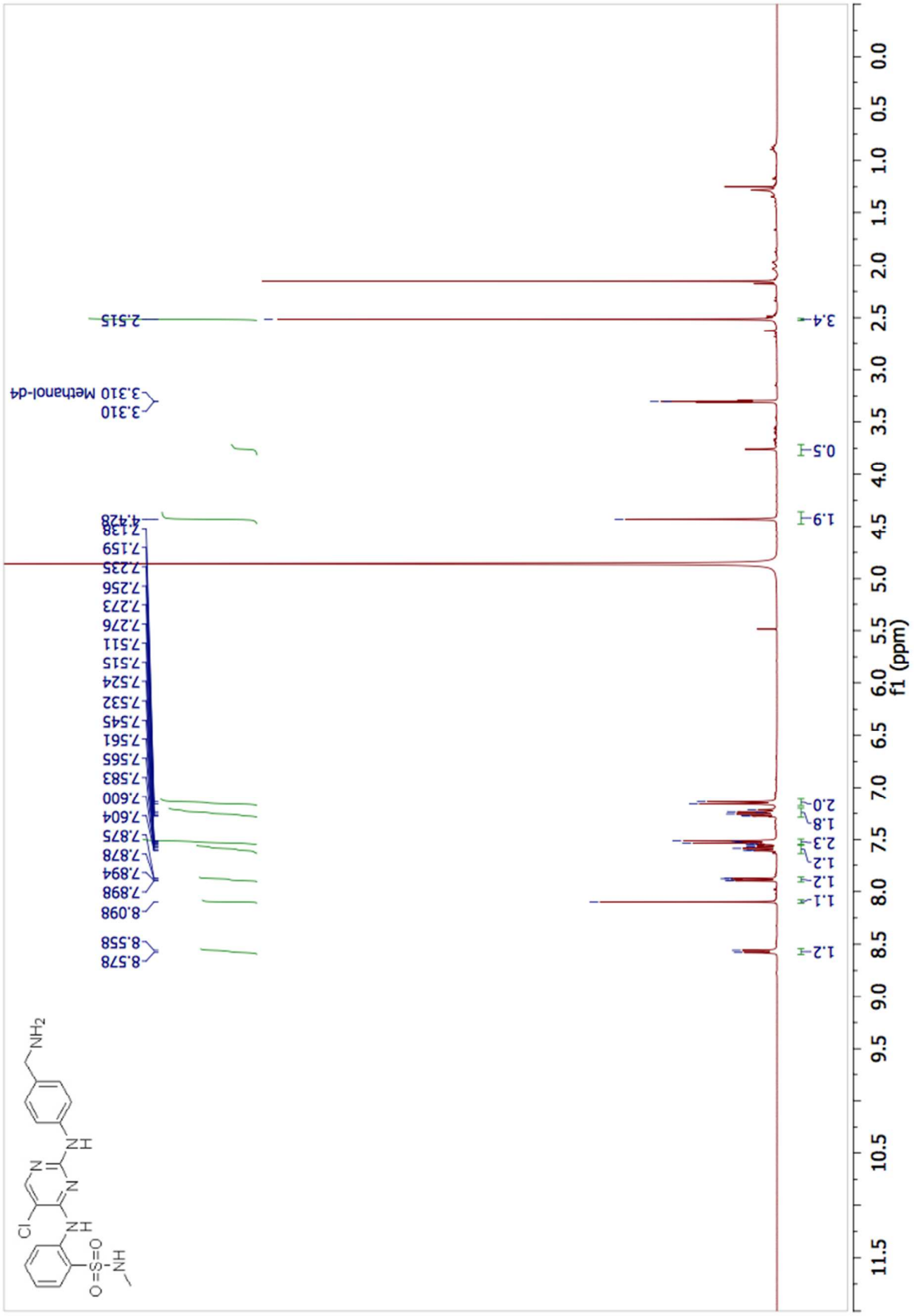

Figure S43: ^{1}H NMR spectrum of **10**.

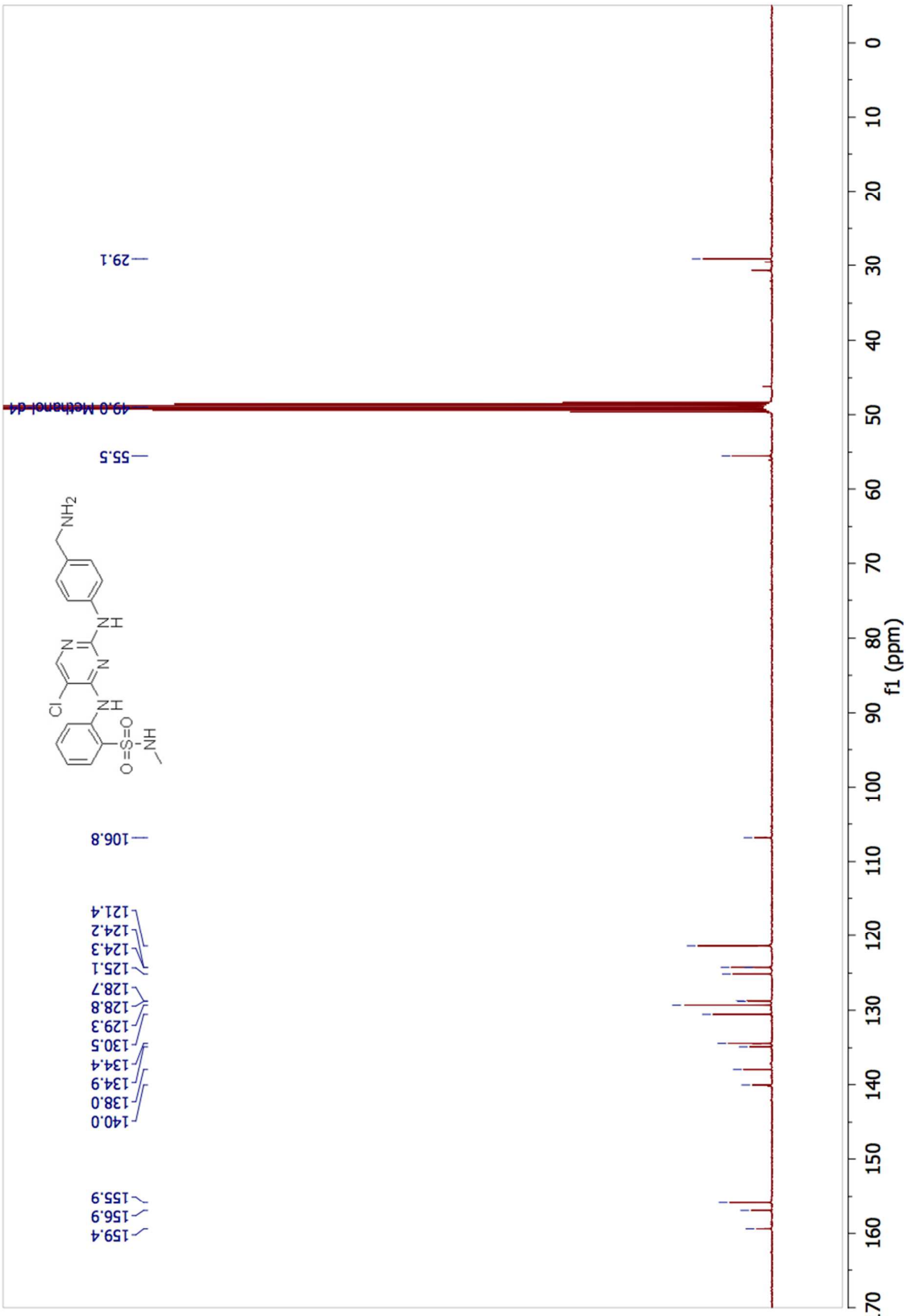

Figure S44: ^{13}C NMR spectrum of **10**.

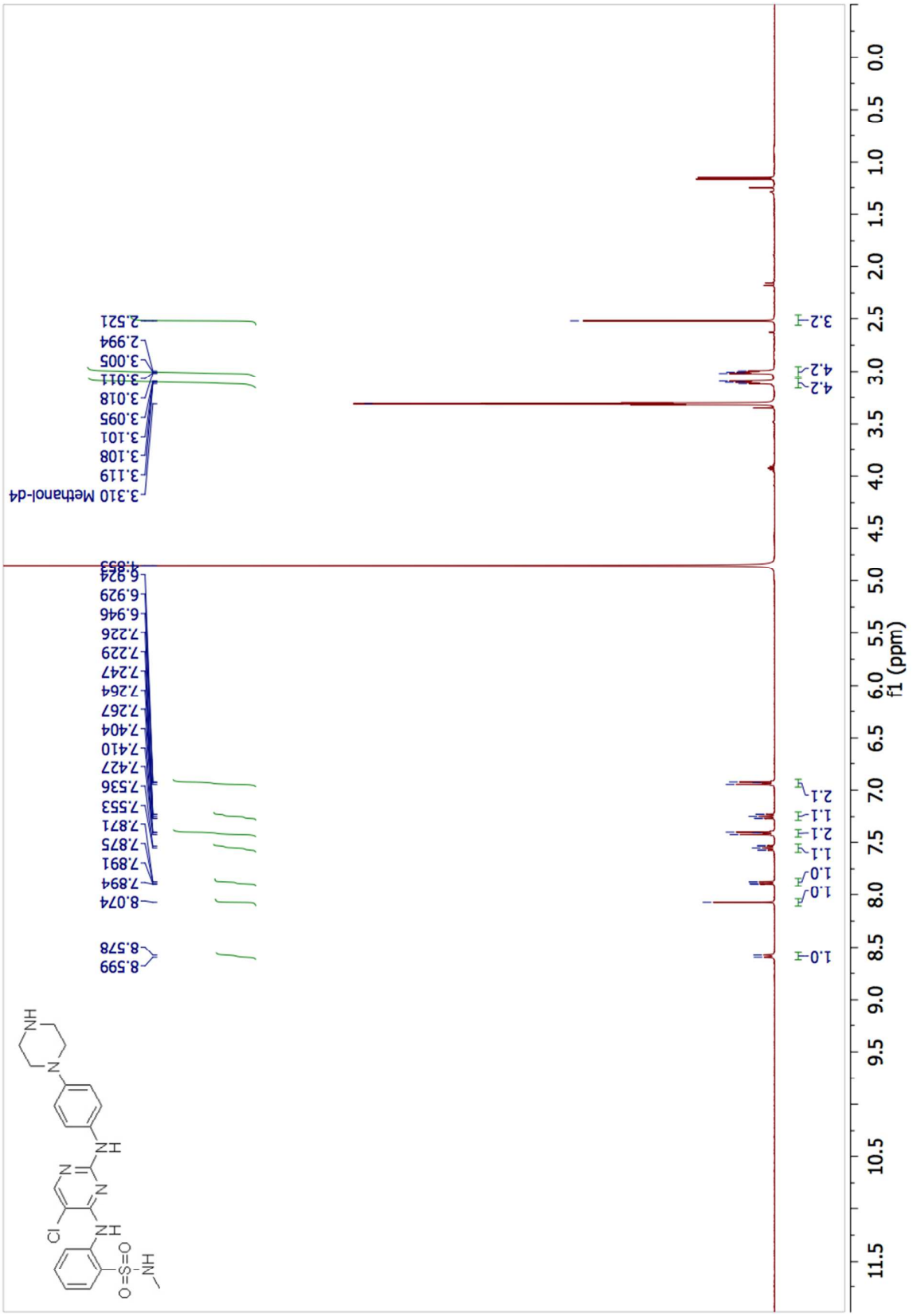

Figure S45: ^{1}H NMR spectrum of **15**.

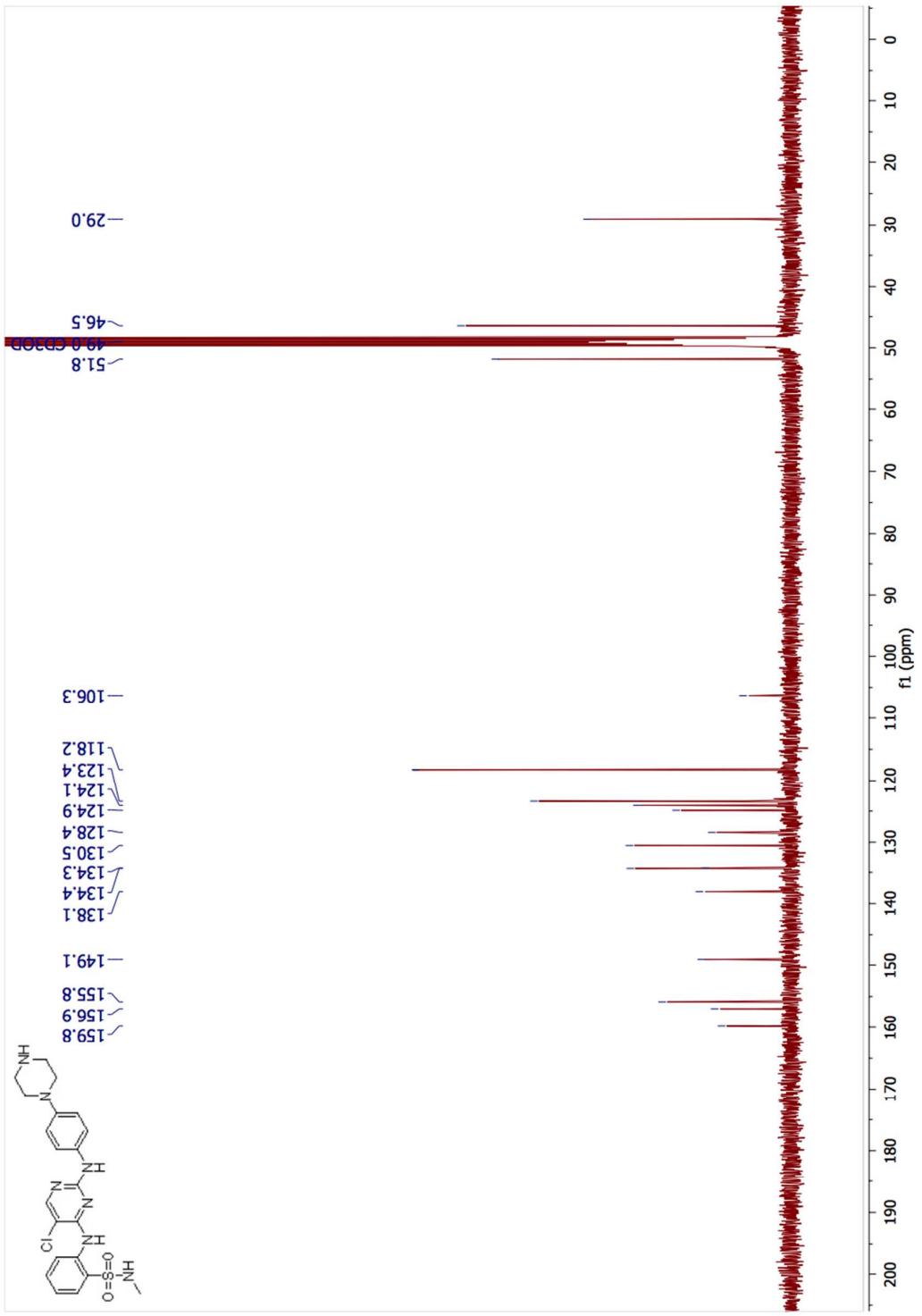

Figure S46: ^{13}C NMR spectrum of **15**.

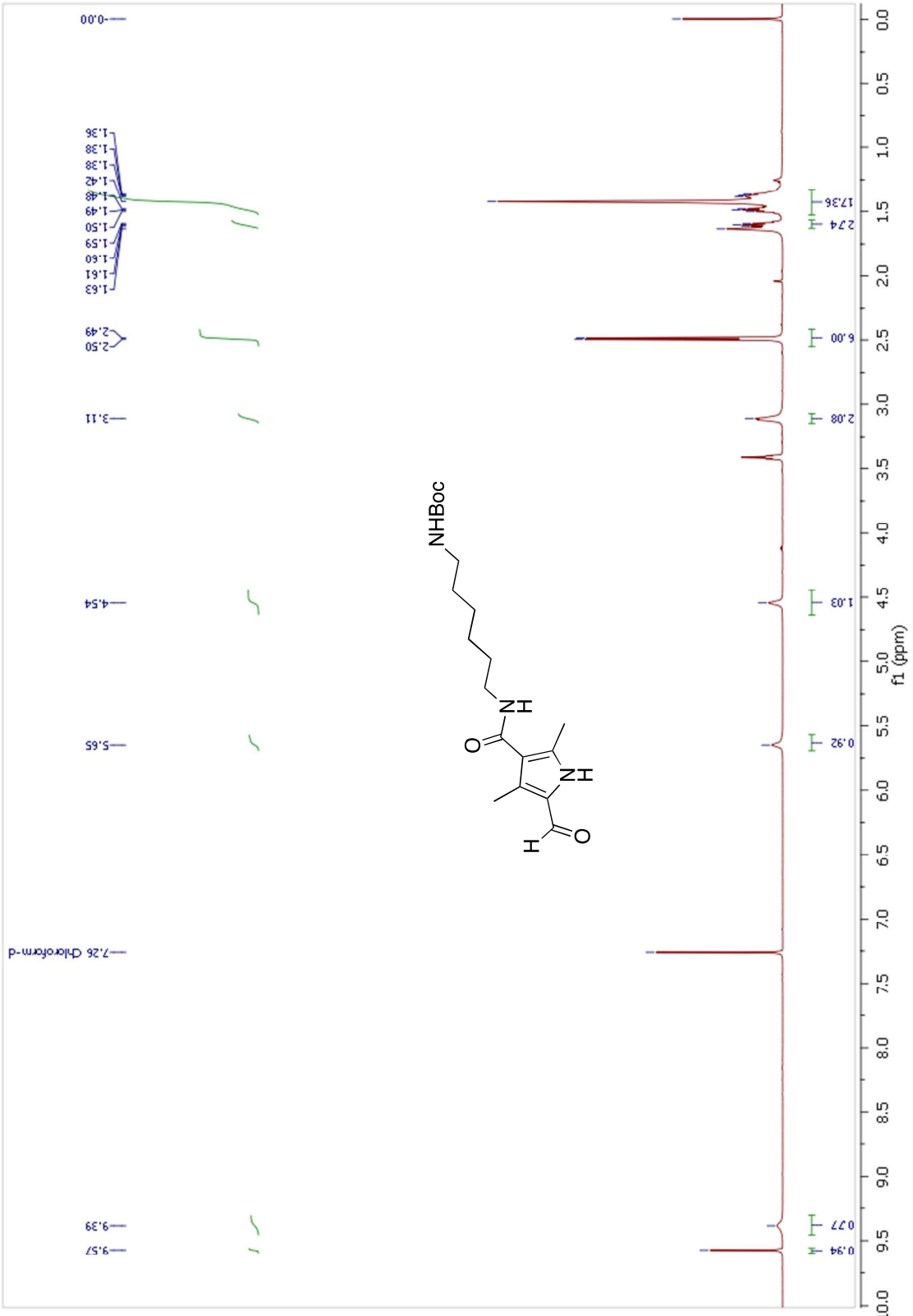

Figure S47: ^{1}H NMR spectrum of *tert*-butyl (6-(5-formyl-2,4-dimethyl-1*H*-pyrrole-3-carboxamido)hexyl)carbamate

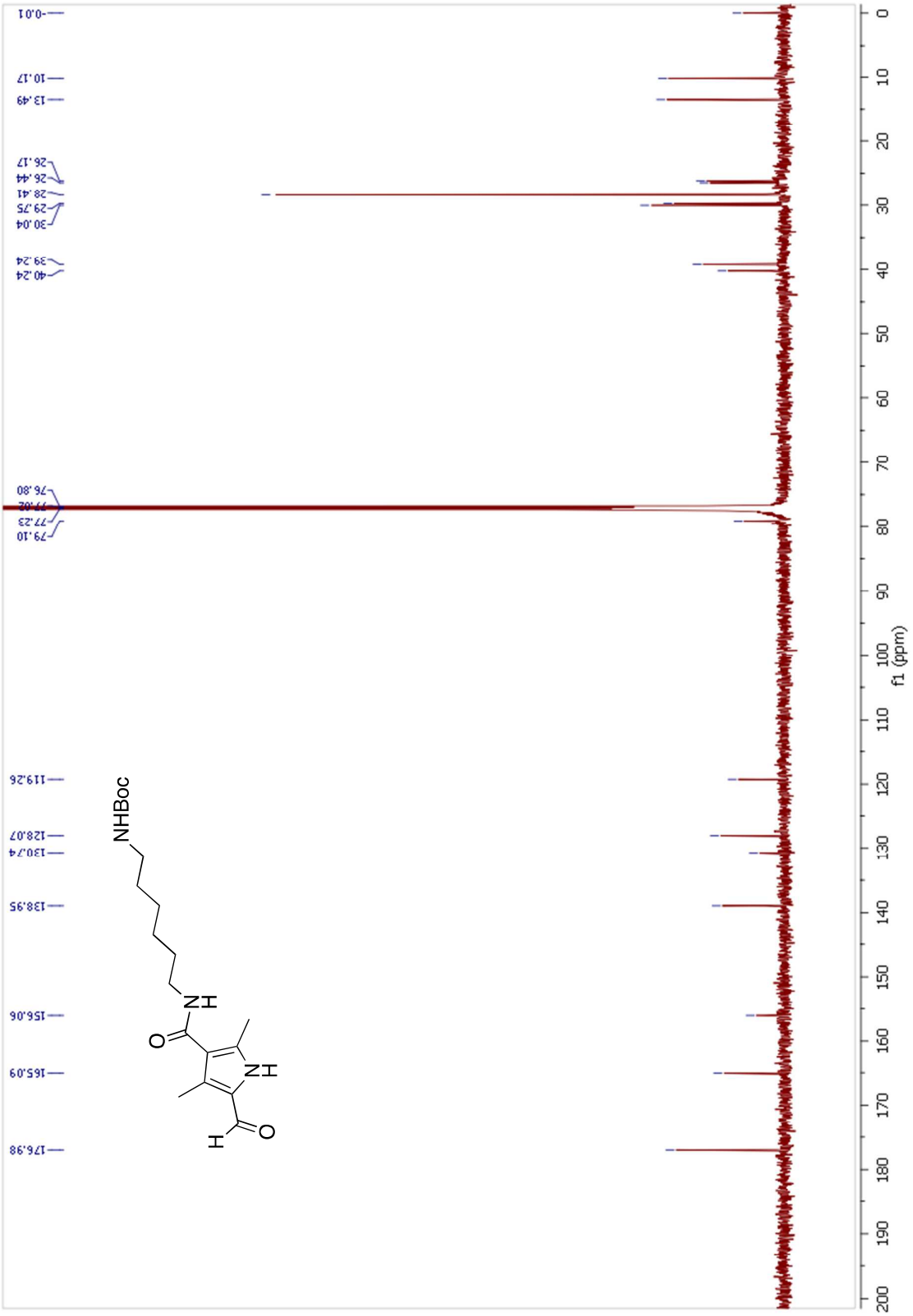

Figure S48: ^{13}C NMR spectrum of *tert*-butyl (6-(5-formyl-2,4-dimethyl-1*H*-pyrrole-3-carboxamido)hexyl)carbamate

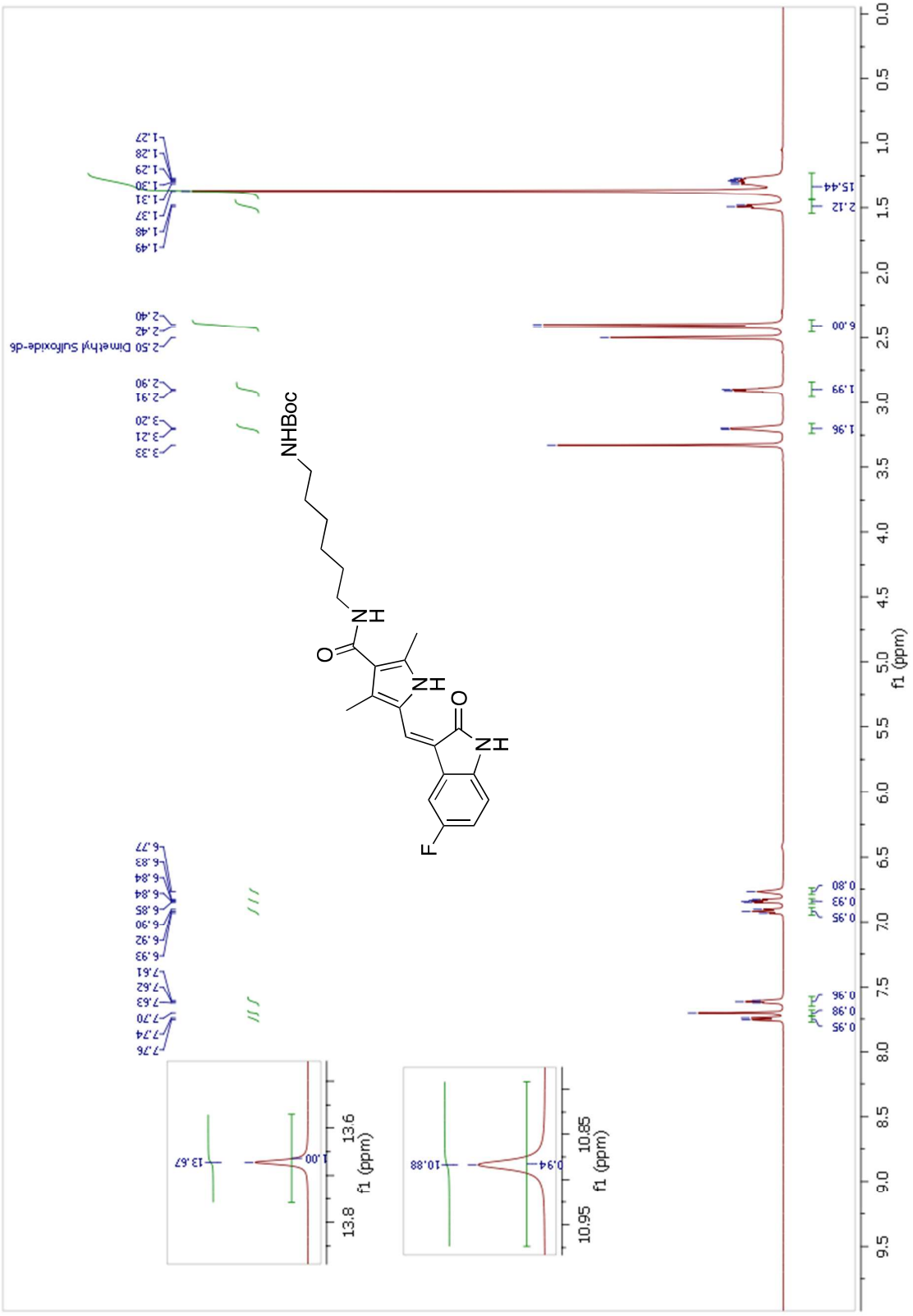

Figure S49: ^{1}H NMR spectrum of (*Z*)-*tert*-butyl (6-(5-((5-fluoro-2-oxoindolin-3-ylidene)methyl)-2,4-dimethyl-1*H*-pyrrole-3-carboxamido)hexyl)carbamate

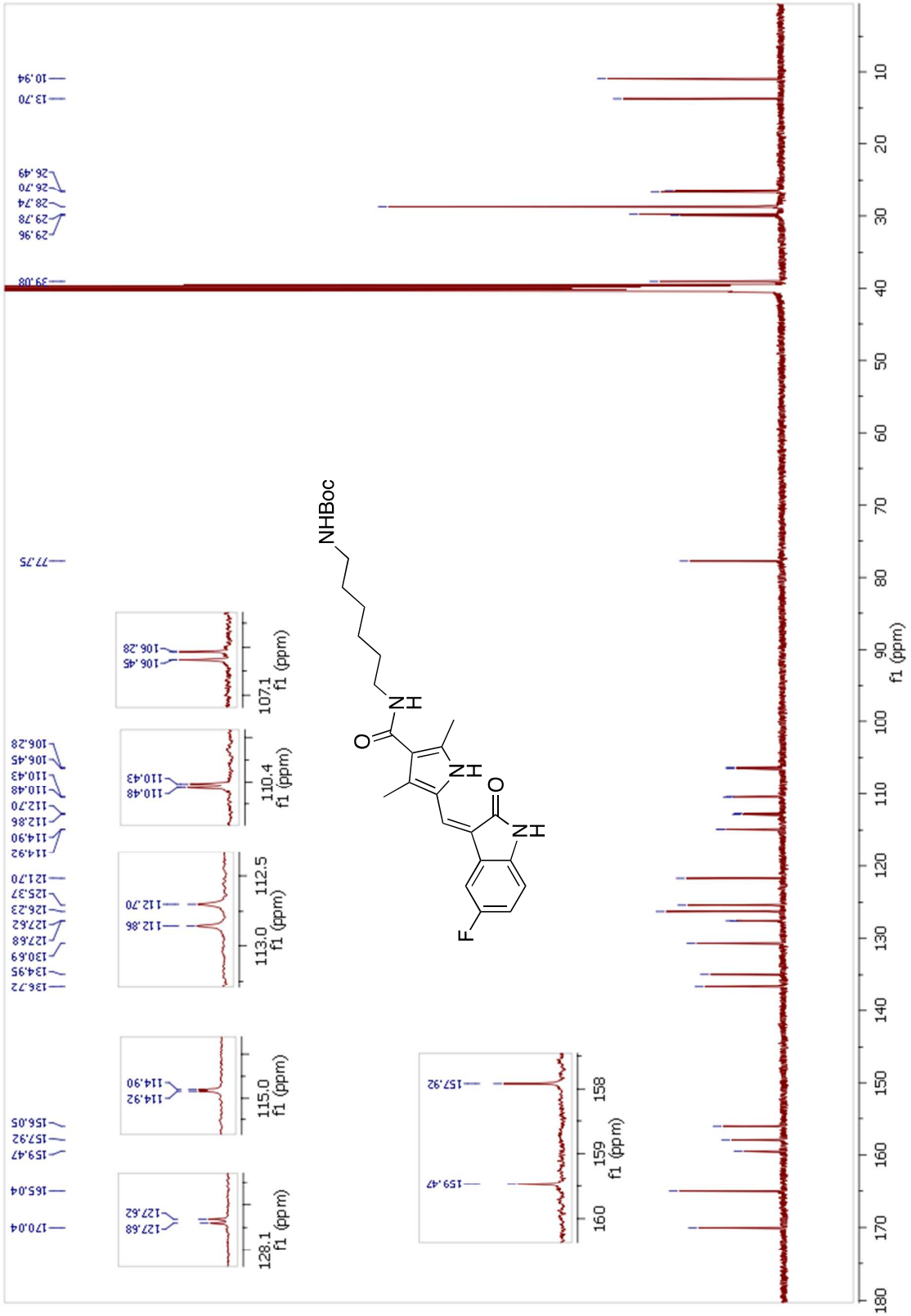

Figure S50: ^{13}C NMR spectrum of (*Z*)-*tert*-butyl (6-(5-((5-fluoro-2-oxoindolin-3-ylidene)methyl)-2,4-dimethyl-1*H*-pyrrole-3-carboxamido)hexyl)carbamate

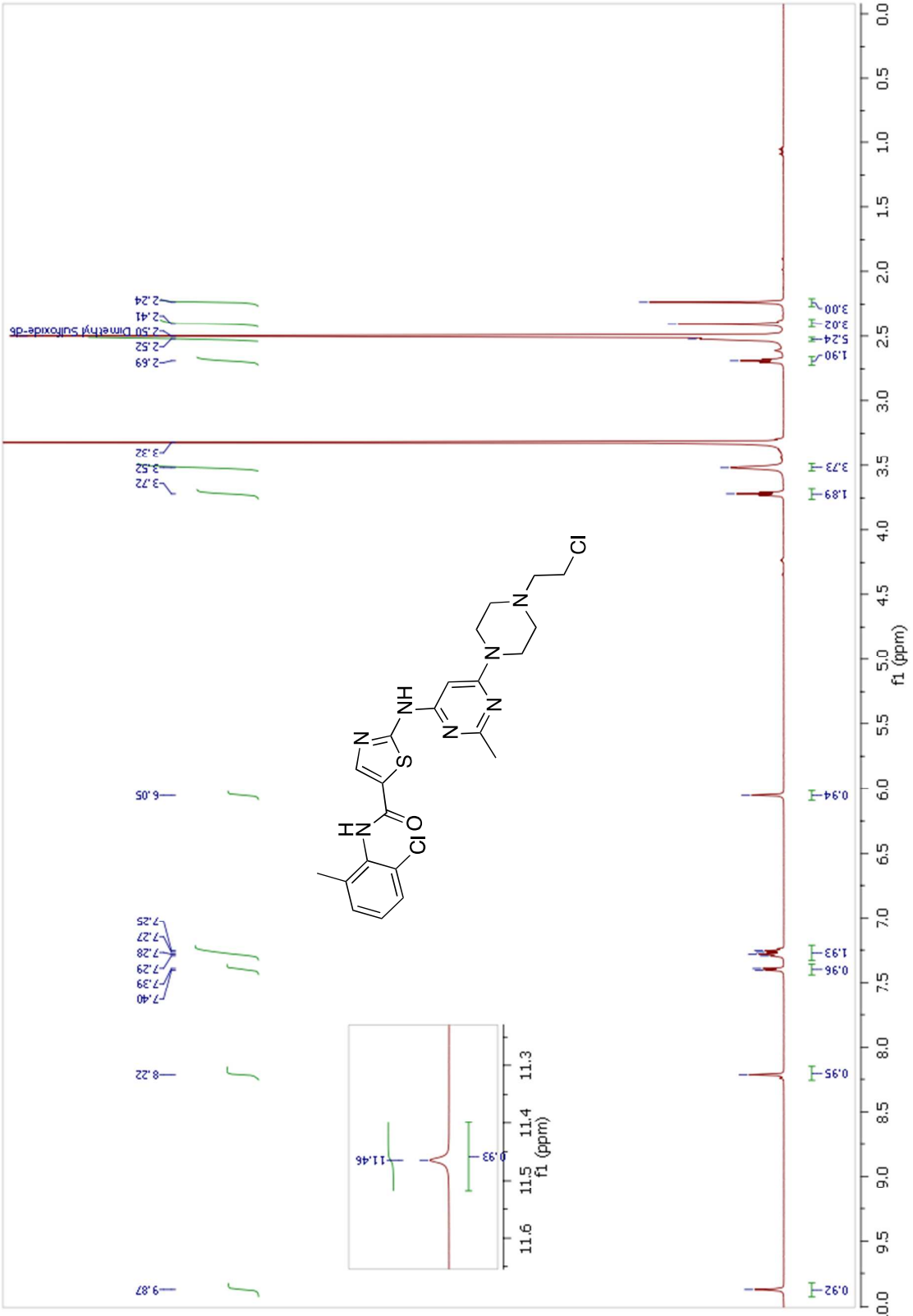

Figure S51: ^{1}H NMR spectrum of *N*-(2-chloro-6-methylphenyl)-2-((6-(4-(2-chloroethyl)piperazin-1-yl)-2-methylpyrimidin-4-yl)amino)thiazole-5-carboxamide

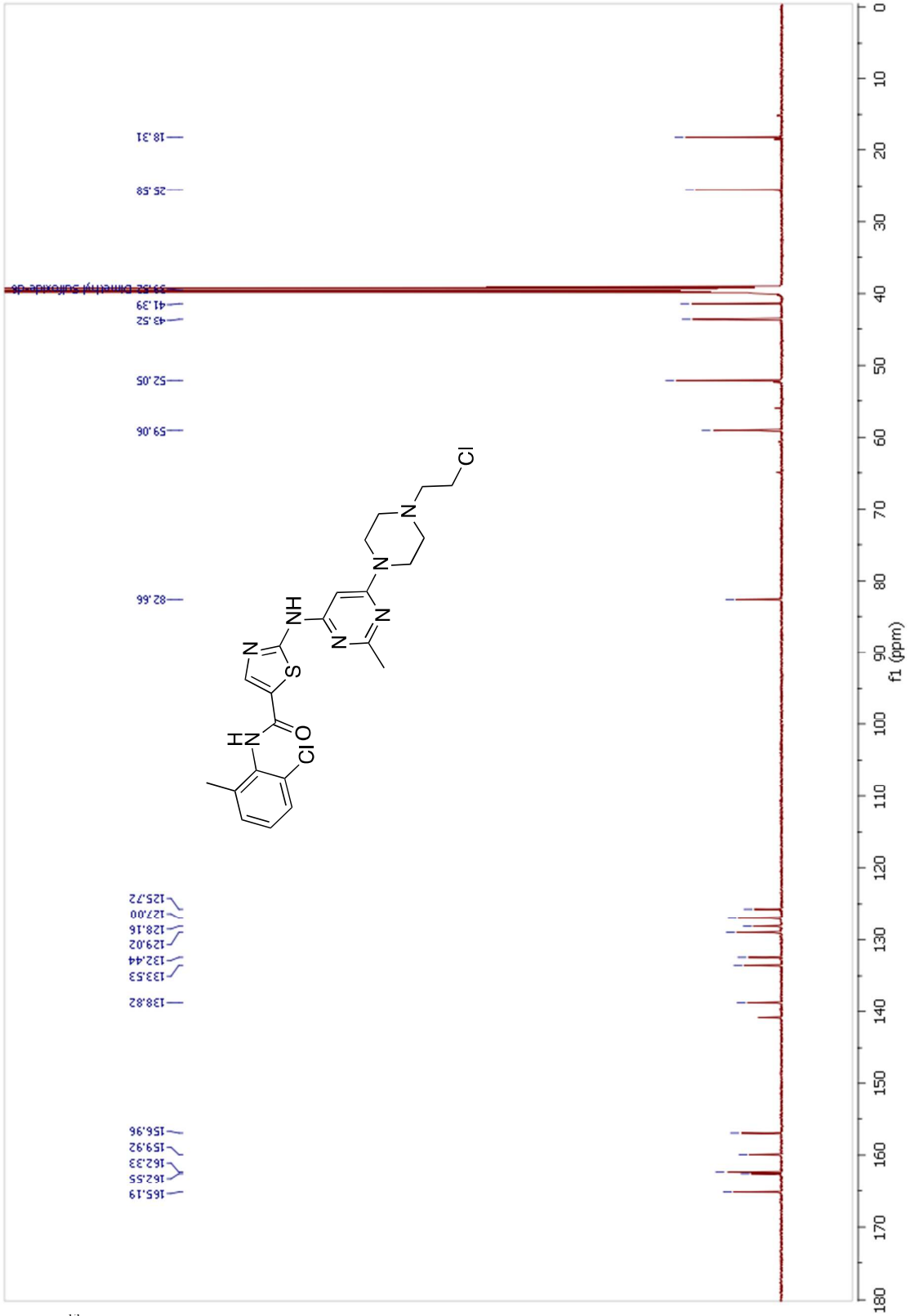

Figure S52: ^{13}C NMR spectrum of *N*-(2-chloro-6-methylphenyl)-2-((6-(4-(2-chloroethyl)piperazin-1-yl)-2-methylpyrimidin-4-yl)amino)thiazole-5-carboxamide

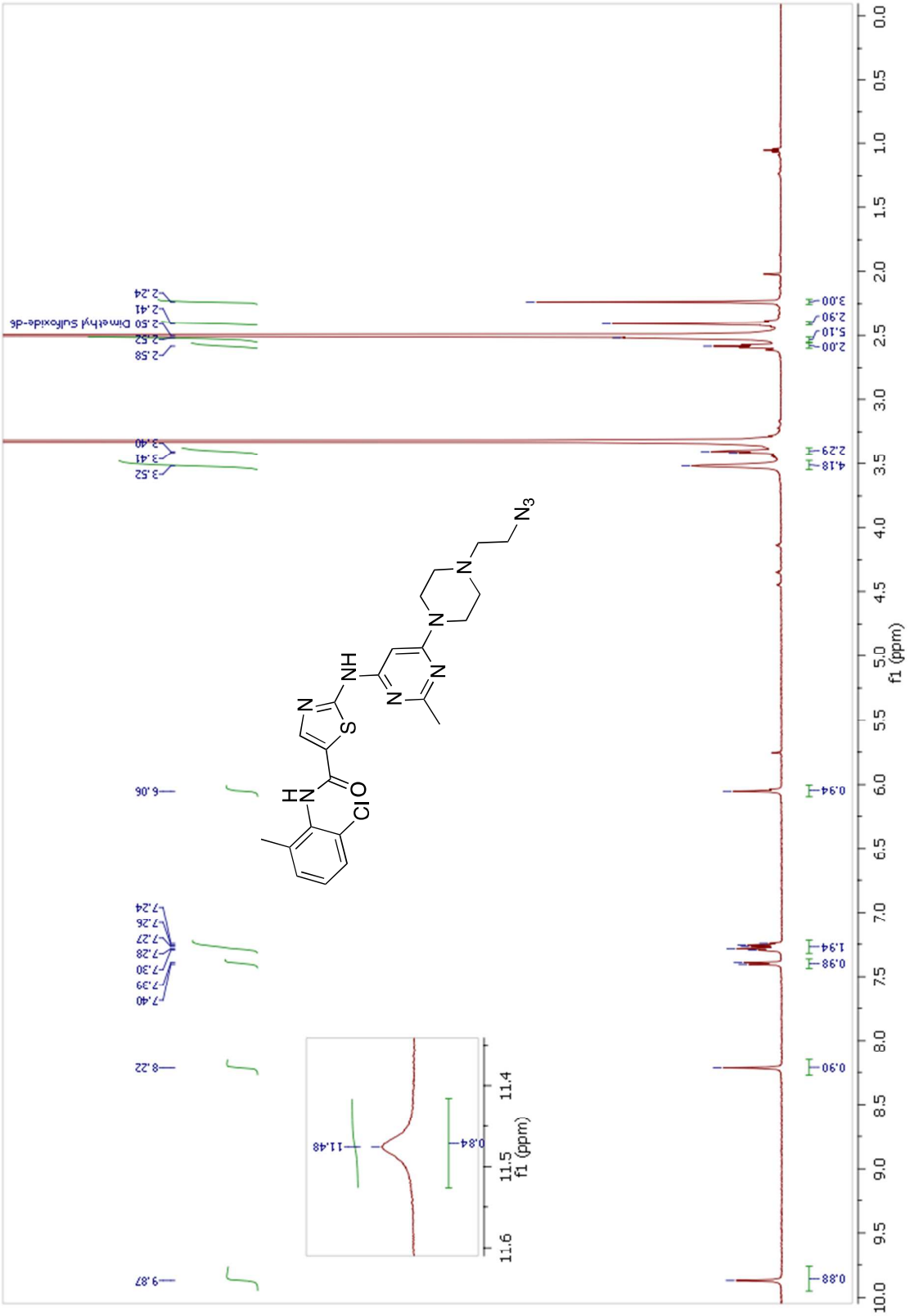

Figure S53: ^{1}H NMR spectrum of 2-((6-(4-(2-azidoethyl)piperazin-1-yl)-2-methylpyrimidin-4-yl)amino)-*N*-(2-chloro-6-methylphenyl)thiazole-5-carboxamide

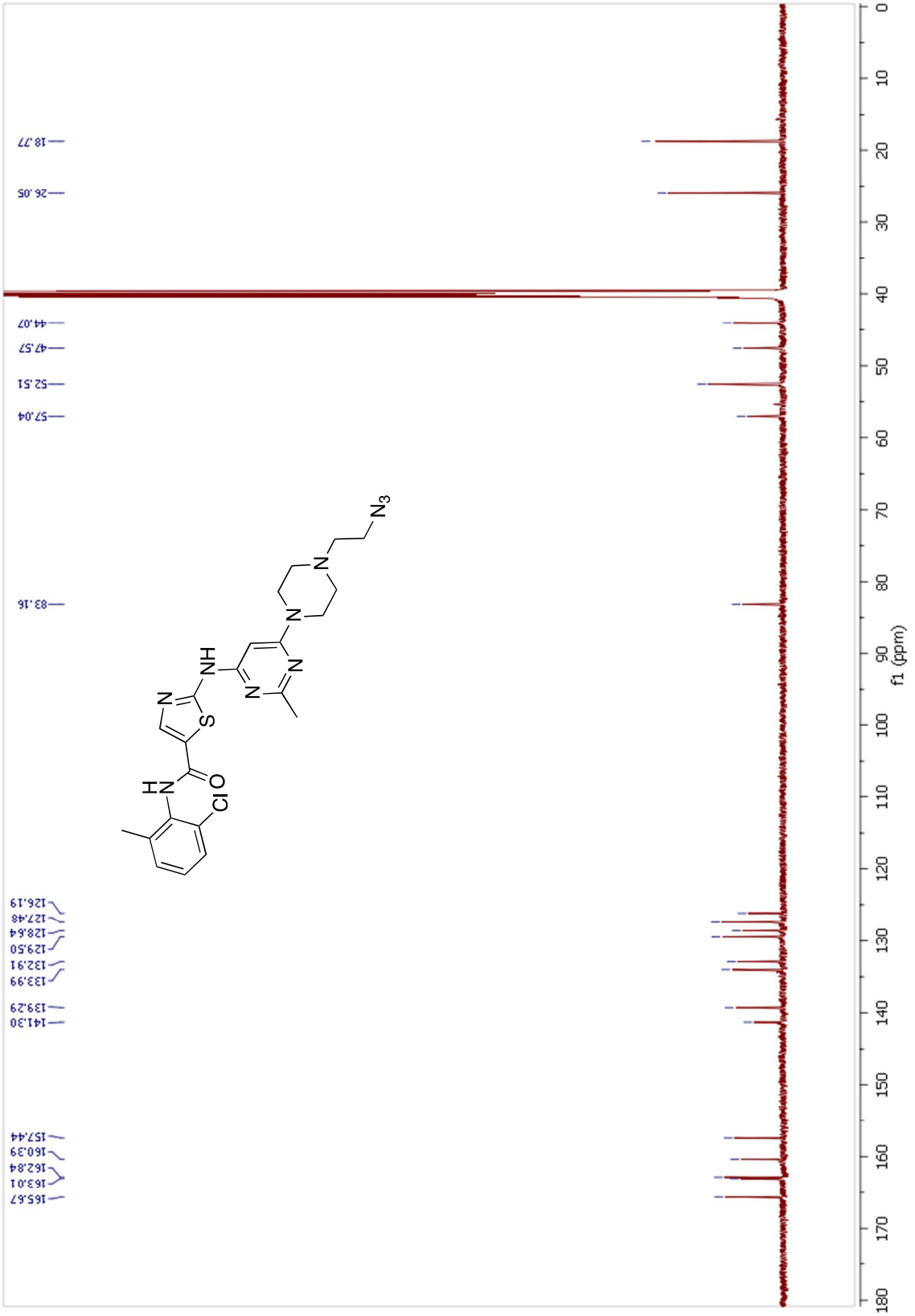

Figure S54: ^{13}C NMR spectrum of 2-((6-(4-(2-azidoethyl)piperazin-1-yl)-2-methylpyrimidin-4-yl)amino)-*N*-(2-chloro-6-methylphenyl)thiazole-5-carboxamide

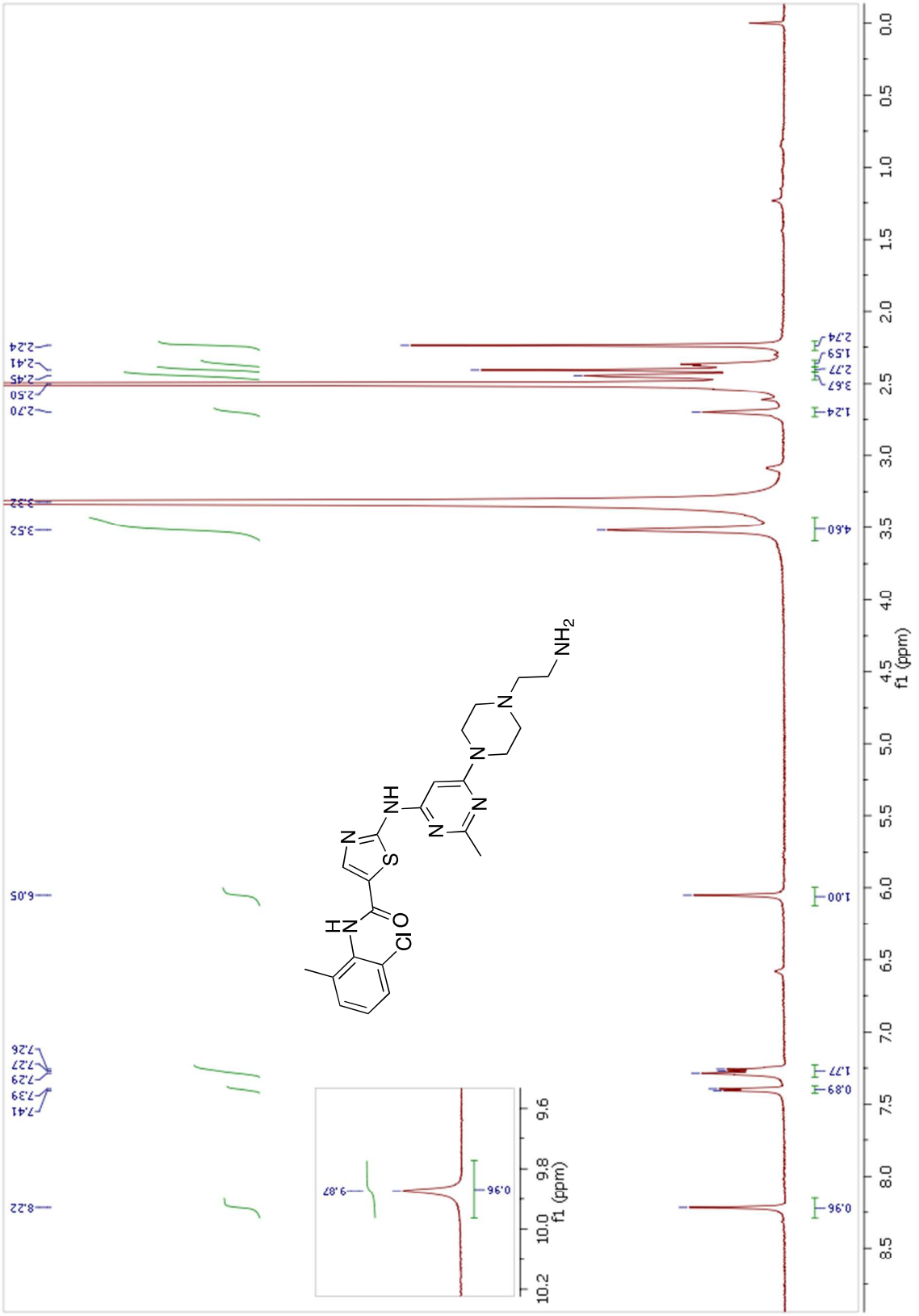

Figure S55: ^{1}H NMR spectrum of 2-((6-(4-(2-aminoethyl)piperazin-1-yl)-2-methylpyrimidin-4-yl)amino)-*N*-(2-chloro-6-methylphenyl)thiazole-5-carboxamide

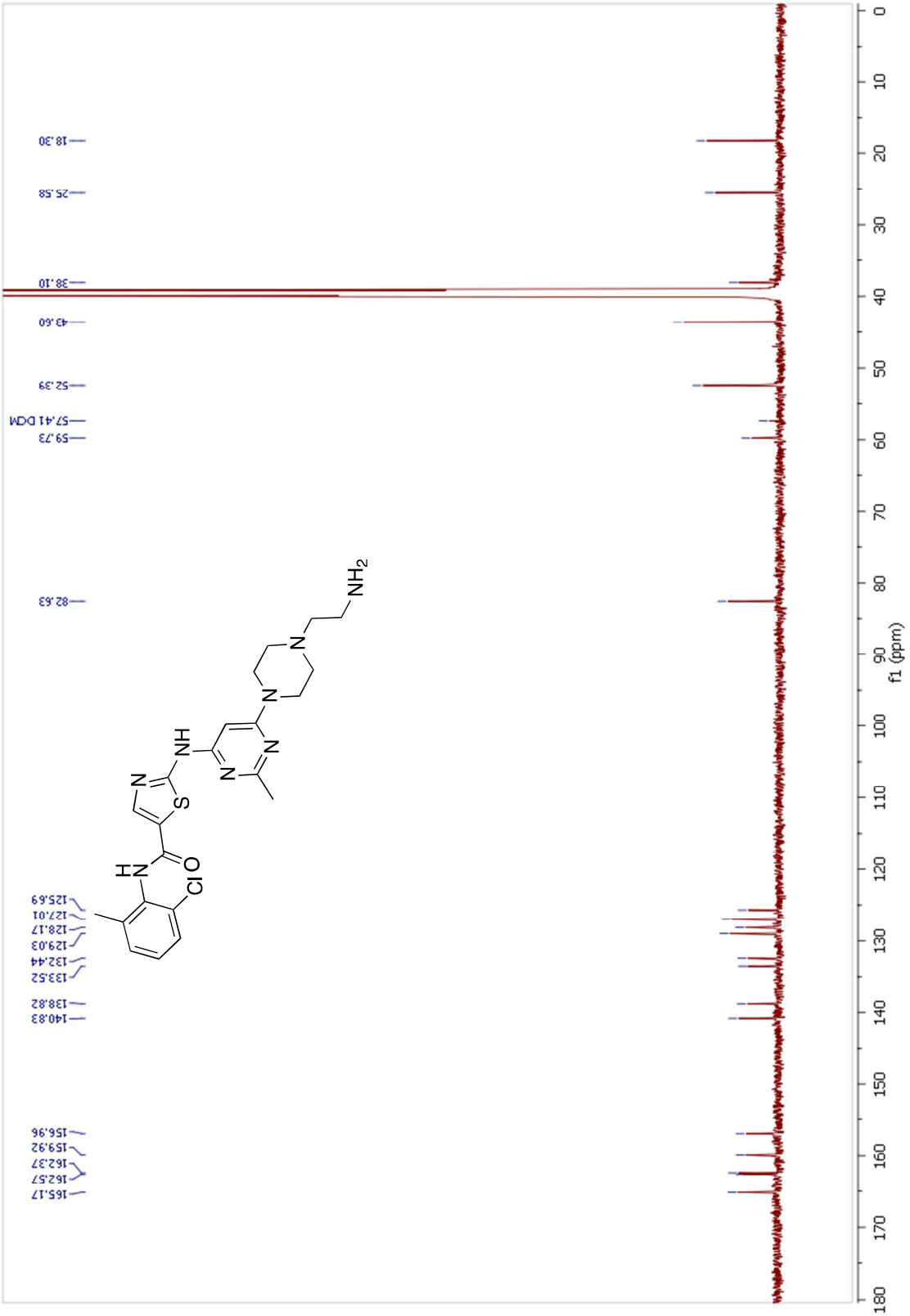

Figure S56: ^{13}C NMR spectrum of 2-((6-(4-(2-aminoethyl)piperazin-1-yl)-2-methylpyrimidin-4-yl)amino)-*N*-(2-chloro-6-methylphenyl)thiazole-5-carboxamide

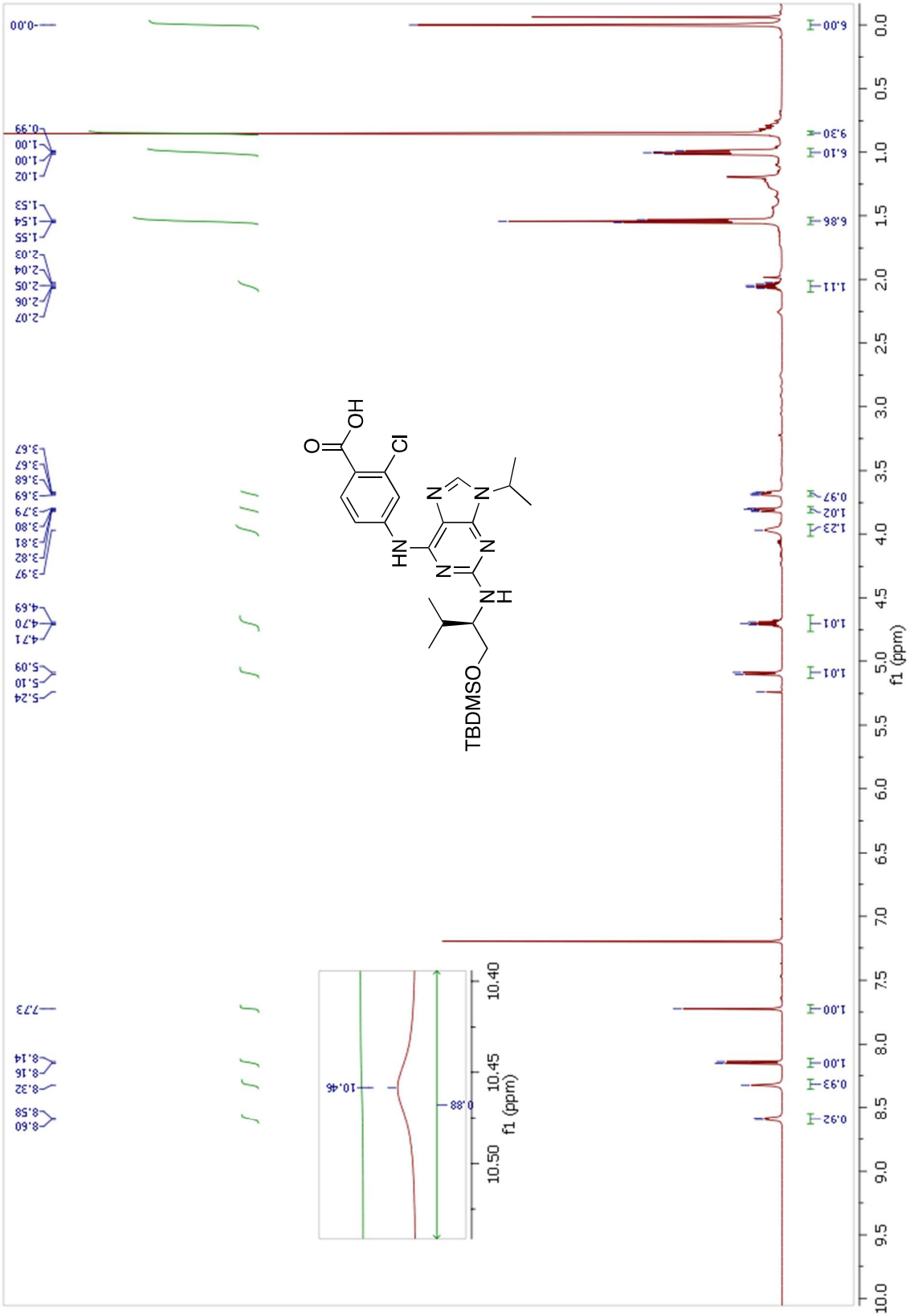

Figure S57: ^{1}H NMR spectrum of (*R*)-4-((2-((1-((tert-butyldimethylsilyl)oxy)-3-methylbutan-2-yl)amino)-9-isopropyl-9*H*-purin-6-yl)amino)-2-chlorobenzoic acid [*O*-TBDMS purvalanol B]

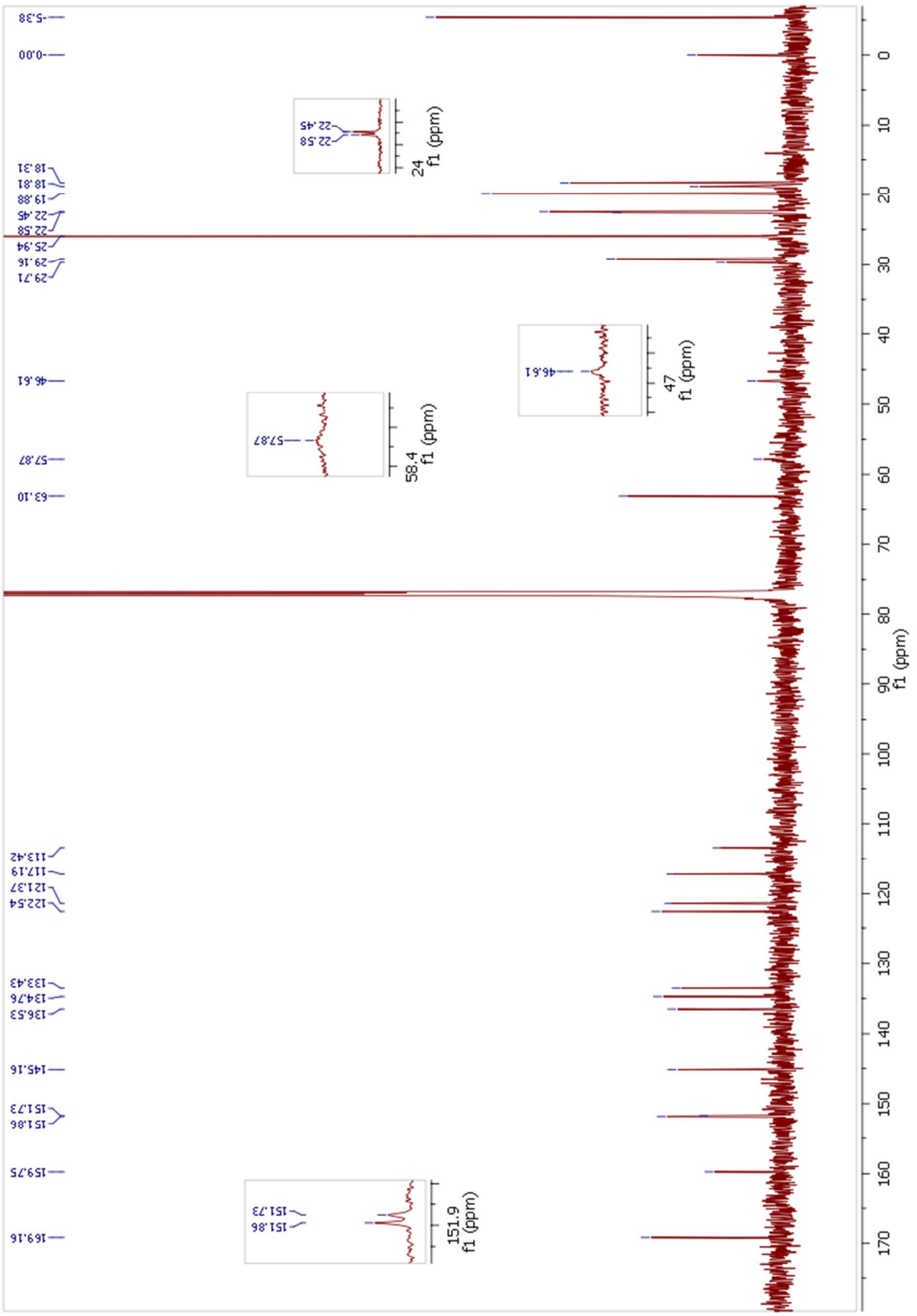

Figure S58: ^{13}C NMR spectrum of (*R*)-4-((2-((1-((tert-butyldimethylsilyl)oxy)-3-methylbutan-2-yl)amino)-9-isopropyl-9*H*-purin-6-yl)amino)-2-chlorobenzoic acid [*O*-TBDMS purvalanol B]

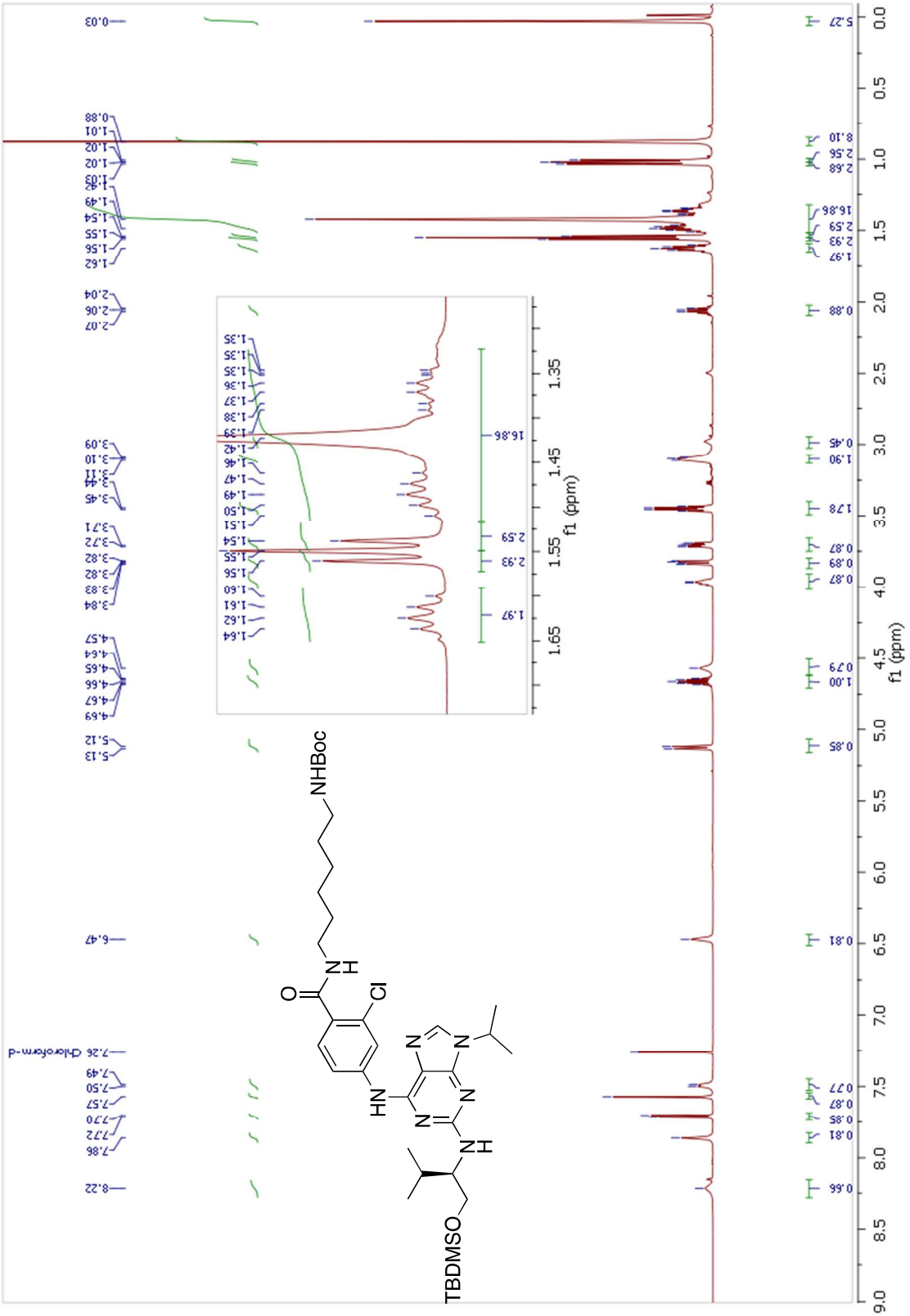

Figure S59: ^{1}H NMR spectrum of (*R*)-*tert*-butyl (6-(4-((2-((1-((tert-butyldimethylsilyl)oxy)-3-methylbutan-2-yl)amino)-9-isopropyl-9*H*-purin-6-yl)amino)-2-chlorobenzamido)hexyl)carbamate

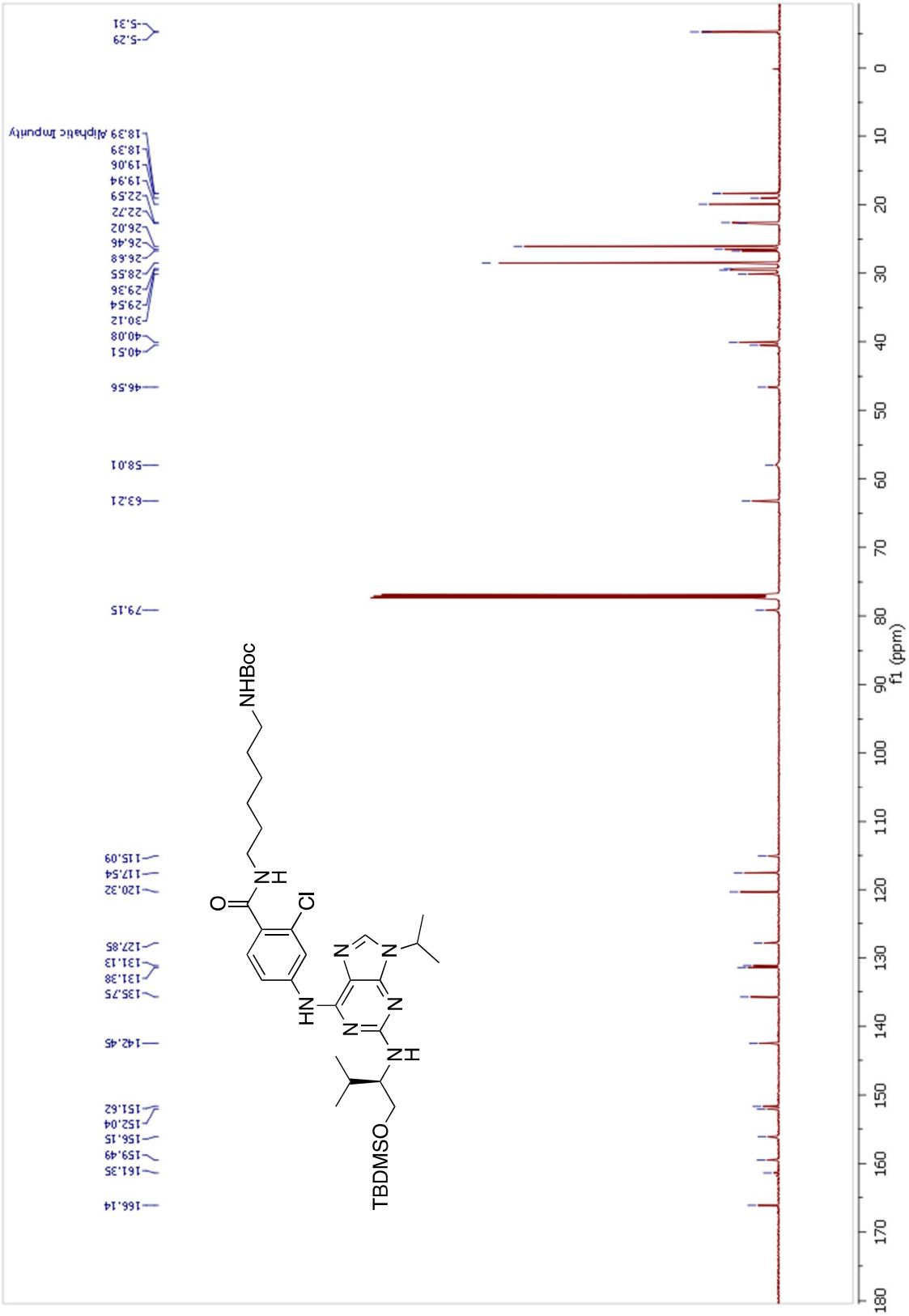

Figure S60: ^{13}C NMR spectrum of (*R*)-*tert*-butyl (6-(4-((2-(((1-((tert-butyldimethylsilyl)oxy)-3-methylbutan-2-yl)amino)-9-isopropyl-9*H*-purin-6-yl)amino)-2-chlorobenzamido)hexyl)carbamate

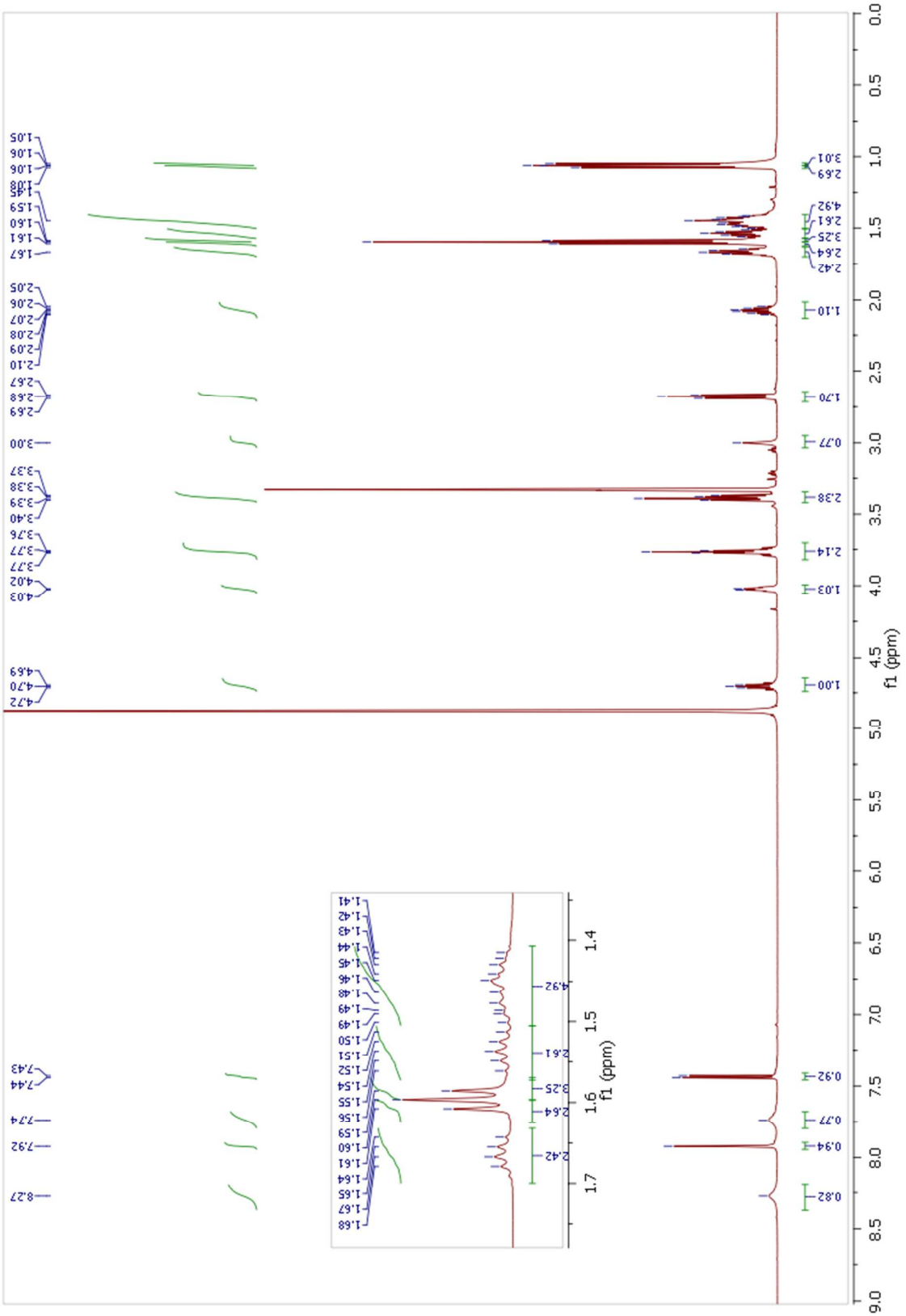

Figure S61: ^{1}H NMR spectrum of (*R*)-N-(6-aminohexyl)-2-chloro-4-((2-((1-hydroxy-3-methylbutan-2-yl)amino)-9-isopropyl-9*H*-purin-6-yl)amino)benzamide

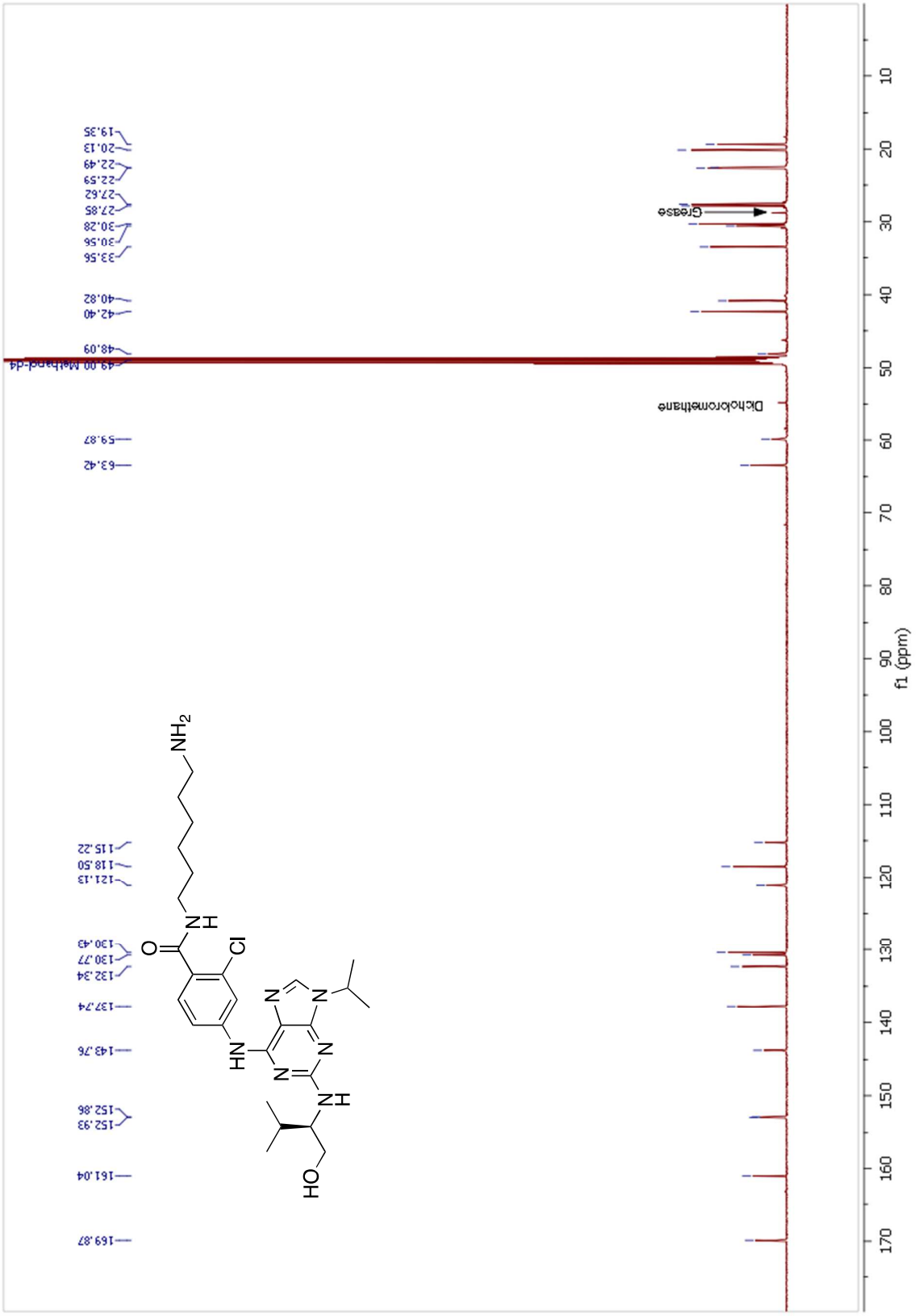

Figure S62: ^{13}C NMR spectrum of (*R*)-N-(6-aminohexyl)-2-chloro-4-((2-((1-hydroxy-3-methylbutan-2-yl)amino)-9-isopropyl-9*H*-purin-6-yl)amino)benzamide